

C-RAN Zero-Forcing with Imperfect CSI: Analysis and Precode&Quantize Feedback

Niv Arad, *Student Member, IEEE*, and Yair Noam, *Member, IEEE*

Abstract

Downlink joint transmission by a cluster of remote radio heads (RRHs) is an essential technique for enhancing throughput in future cellular networks. This method requires global channel state information (CSI) at the processing unit that designs the joint precoder. To this end, a large amount of CSI must be shared between the RRHs and that unit. This paper proposes two contributions. The first is a new upper bound on the rate loss, which implies a lower bound on the achievable rate, obtained by a cluster of RRHs that employ joint zero-forcing (ZF) with incomplete CSI. The second contribution, which follows insights from the bound, is a new CSI sharing scheme that drastically reduces the large overhead associated with acquiring global CSI for joint transmission. In a nutshell, each RRH applies a local precoding matrix that creates low-dimensional effective channels that can be quantized more accurately with fewer bits, thereby reducing the overhead of sharing CSI. In addition to the CSI sharing-overhead, this scheme reduces the data rate that must be delivered to each RRH in the cluster.

Index Terms

Broadcast channel, multiple-input multiple-output (MIMO), joint transmission (JT), cloud radio-access network (C-RAN), 5G, finite rate feedback, zero-forcing, beamforming, lower bound.

I. INTRODUCTION

Joint transmission (JT) in which adjacent cellular transmitters form a cluster that serves multiple mobile stations (MSs) is a key strategy for enhancing spectrum utilization. The idea is to transform interference between adjacent cells into useful signals (see [2] and references

N. Arad and Y. Noam are with the Faculty of Engineering, Bar-Ilan University, Ramat-Gan, 5290002 Israel (e-mail: nivarad44@gmail.com; yair.noam@biu.ac.il). Some of the results reported here appeared in [1]. This research was supported by an Israel Ministry of Science “Kamin” grant.

therein). To do so, transmitters in the cluster must share both the data and CSI. Such a high level of cooperation is the main obstacle to exploiting the vast potential of JT in practice.

The upcoming mobile fifth generation (5G) technology includes several new features that facilitate inter-cell cooperation. The most important is the cloud radio-access network (C-RAN) architecture in which a centralized base-band unit (BBU) pool is connected via high data-rate links, dubbed *fronthaul*, to a large number of RRHs [3, 4]. A fully centralized C-RAN carries out all the digital processing by the BBU pool, which requires a low-latency, ultra-wide bandwidth fronthaul that is not always feasible. This can be solved by a more functional RRH, dubbed smart RRH (S-RRH), which carries out some of the digital processing [5–7], especially tasks that require low latency. The heavy processing, such as coding and decoding, will be done at the BBU.

Nevertheless, JT remains a challenging task. The fronthaul data rate between the BBU and each S-RRH is proportional to the number of users in the cluster. Supporting such a rate may be difficult. Another problem is related to CSI and fronthaul latency. In JT, each S-RRH quantizes the CSI and feeds it back to the BBU to calculate the joint precoding matrix. This matrix is then quantized and fed backward to the S-RRHs, forming the cluster. The entire process must be completed within a few milliseconds; otherwise, the beamformer becomes outdated. If the fronthaul does not support this latency, the joint precoding-matrix calculation must be carried out by a central unit (CU) that is interconnected to the cooperating S-RRHs via a low-latency link, dubbed Xn,¹ which may be separate from the fronthaul. However, while the Xn-link is low latency, it may be rate-limited; a factor that decreases the CSI accuracy at the CU and has an extremely negative effect on the performance of JT, which is highly sensitive to inaccurate CSI.

Downlink transmission with perfect and imperfect CSI by a single transmitter [9–11] as well as with multiple transmitters employing JT [2, 12–18] is an important, well-studied topic. Imperfect CSI may result from the limited wireless feedback-channel between MSs to the transmitters [11–14]. We focus on a different case where there is channel reciprocity (e.g., time division duplex). Thus, the limiting factor is the connection between S-RRHs in the cluster. An important line of research has dealt with reducing the fronthaul data rate [15–18]. Here, in addition to reducing the

¹Without restricting ourselves to a particular standard, we use the term Xn, used in 5G [8] for the link that interconnects S-RRHs.

fronthaul data rate, we deal with another issue; namely JT with imperfect CSI. There are different approaches to reducing JT CSI-overhead. One method, used in uplink JT, compresses the CSI delivered to the CU [19]. Another approach is robust (to inaccurate CSI) precoding [20, 21]. Other methods feed back only a subset of the channels (e.g. [22, 23]), or use compressive CSI acquisition [24].

This paper considers a cluster of S-RRHs that employ downlink linear-precoding JT under single user decoding (SUD) at the receivers; i.e., each MS treats the signals intended for other MSs as noise. We further assume channel reciprocity; thus, each S-RRH has perfect local CSI concerning all the MSs in the cluster.

The paper presents two contributions. The first is a new upper-bound on the rate-loss when the CU sets the overall joint-ZF precoding matrix using imperfect CSI (cf. Fig. 1) compared to perfect CSI. The latter bound can be used to obtain a lower bound on the achievable rate. We assume that each S-RRH quantizes its local CSI using random vector quantization (RVQ) [25]. Similar bounds for the broadcast channel with imperfect CSI can be found in [9, 26]. The proposed bound differs from previous ones by the type of imperfect CSI; i.e., it considers JT in which the cooperating transmitters (S-RRHs) have limited interconnecting links. Each user's channel is quantized as a haul in the former bounds, whereas here, in sub-blocks. This sub-block quantization induces an entirely different CSI error distribution.

The second contribution is a new scheme for precoding and CSI sharing, dubbed precode and quantize (P&Q), which has two advantages. First, it reduces the number of CSI quantization bits transferred on the Xn-link between the S-RRHs and the CU. The second advantage is that it reduces the overall fronthaul data rate between the S-RRHs and the BBU. A key distinguishing characteristic of this scheme is that it applies front-end precoding matrices at the S-RRHs prior to CSI quantization. These matrices aim at improving CSI accuracy at the CU. Each S-RRH autonomously calculates and applies a matrix, based on its local CSI, and creates an effective channel of lower dimensionality that can be quantized more accurately. These channels are then quantized and sent to the CU, which in turn calculates a joint precoding matrix and feeds it back to the S-RRHs. We show, both theoretically and numerically, that this scheme significantly increases the network throughput compared to the standard scheme, where each S-RRH quantizes its local CSI and feeds it back to the CU. This performance gain is maintained for a wide range of CSI quantization bits and SNR. Equally important, the proposed feedback scheme provides

a significant reduction in the data load on the fronthaul connecting the S-RRHs and the BBU.

The remainder of this paper is organized as follows. Sec. II introduces the system model. In Sec. III, a new upper-bound on the rate-loss is presented. Sec. IV describes the P&Q CSI sharing scheme and its benefits while Sec. V analyzes its performance theoretically. Simulation results are given in Sec. VI and conclusions in Sec. VII.

Notation: Boldface lower (upper) case letters denote vectors (matrices). $(\cdot)^*$ and $(\cdot)^\dagger$ denote the conjugate and the conjugate transpose operations, respectively. Moreover, \odot and \otimes denote the Hadamard and Kronecker products, respectively. Let \mathbf{a} , be a vector, then $\bar{\mathbf{a}}$ denotes its normalized version; i.e., $\bar{\mathbf{a}} = \mathbf{a}/\|\mathbf{a}\|$. Also, $\angle(\mathbf{a}, \mathbf{b})$ denotes the angle between \mathbf{a} and the vector \mathbf{b} . In addition, let \mathcal{Q} be a set and $q \in \mathcal{Q}$, then $\mathcal{Q}_q = \mathcal{Q} \setminus \{q\}$. Consider $\{\mathbf{A}_q\}_{q=1}^Q$, where $\mathbf{A}_q \in \mathbb{C}^{N \times M}$, then $\mathbf{A} = \text{blockdiag}(\mathbf{A}_1, \dots, \mathbf{A}_Q) \in \mathbb{C}^{QN \times QM}$ denotes the block diagonal matrix, whose q th diagonal-block is equal to \mathbf{A}_q ; i.e., $[\mathbf{A}]_{(q-1)N+n, (q-1)M+m} = [\mathbf{A}_q]_{n,m} \forall 1 \leq q \leq Q, 1 \leq n \leq N, 1 \leq m \leq M$ and is equal to zero otherwise, where $[A]_{l,m}$ denotes the (l, m) entry of \mathbf{A} . Let $\mathcal{H} = \text{span}(\mathbf{h}_1, \dots, \mathbf{h}_M)$, then $\mathbf{P}_{\mathcal{H}}, \mathbf{P}_{\mathcal{H}}^\perp$ denote the projection matrices into space spanned by \mathcal{H} and into its orthogonal complement, respectively. Also, $\chi_{\mathcal{A}}(x)$ represents the indicator function; that is, $\chi_{\mathcal{A}}(x) = 1$ if $x \in \mathcal{A}$ and 0 otherwise, \mathbf{I}_N denotes an $N \times N$ identity matrix and $\mathbf{1}_N, \mathbf{0}_N$ denote an $N \times 1$ vector of ones, and zeros, respectively. Finally, we use \log for the base 2 logarithm.

II. SYSTEM MODEL

Consider a cluster of M S-RRHs, each with N_t antennas, that jointly serve Q single-antenna MSs, as depicted in Fig. 1. We denote the set of S-RRHs $\{1, \dots, M\}$ by \mathcal{M} and the set of MSs $\{1, \dots, Q\}$ by \mathcal{Q} . Assuming flat fading channels, the *downlink* signal, observed by MS- q , is given by

$$y_q = \sum_{m=1}^M \mathbf{h}_{q,m}^\dagger \mathbf{x}_m + n_q, \quad \forall q \in \mathcal{Q} \quad (1)$$

where n_q is an additive, proper-complex Gaussian noise $n_q \sim \mathcal{CN}(0, \sigma_n^2)$, $\mathbf{x}_m \in \mathbb{C}^{N_t \times 1}$ is the signal transmitted by S-RRH- m ; $\mathbf{h}_{q,m} \in \mathbb{C}^{N_t \times 1}$ is the channel between S-RRH- m and MS- q . We further denote

$$\mathbf{h}_q \triangleq [\mathbf{h}_{q,1}^\dagger, \dots, \mathbf{h}_{q,M}^\dagger]^\dagger \in \mathbb{C}^{MN_t \times 1}. \quad (2)$$

Assumption 1: The channels are Rayleigh, independent identically distributed (i.i.d.) block-fading.² Moreover, we assume large-scale fading (e.g. pathloss and shadowing effects), expressed by an attenuation factor $\alpha_{q,m}$. Explicitly, the channel $\mathbf{h}_{q,m} \sim \mathcal{CN}(\mathbf{0}_{N_t}, \alpha_{q,m} \mathbf{I}_{N_t})$, $\forall q \in \mathcal{Q}, m \in \mathcal{M}$ varies at each coherence time, whereas $\alpha_{q,m}$ remains constant during the entire codeword.

Assumption 2: We assume a practically oriented short-time power constraint P_{\max} for each S-RRH; i.e., $\mathbb{E}\{\|\mathbf{x}_m\|^2|U\} \leq P_{\max}$, $\forall m \in \mathcal{M}$ for every coherence-time, where U is the overall instantaneous-CSI. We further assume a linear precoding scheme in which $\mathbf{x}_m = \sum_{q \in \mathcal{Q}} s_q \mathbf{p}_{q,m}$, where $s_q \in \mathbb{C}$ is the information bearing signal intended to MS- q and $\mathbf{p}_{q,m} \in \mathbb{C}^{N_t \times 1}$ is the pre-coding vector from S-RRH- m to MS- q . Finally s_1, \dots, s_q are assumed i.i.d. and $s_q \sim \mathcal{CN}(0, P_q)$.

We focus on a fully cooperative multi-cell system; thus, the joint downlink transmission can be conveniently modeled as a large multiple-input single-output (MISO) broadcast channel with MN_t transmitting antennas [28], such that the signal observed by MS- q can be written as

$$y_q = \mathbf{h}_q^\dagger \mathbf{p}_q s_q + \sum_{j \in \mathcal{Q} \setminus \{q\}} \mathbf{h}_q^\dagger \mathbf{p}_j s_j + n_q, \quad \forall q \in \mathcal{Q} \quad (3)$$

where $\mathbb{E}\{|s_q|^2\} = P_q$, $\|\mathbf{p}_q\|^2 = 1$ and \mathbf{p}_q is the overall joint beamforming vector designated for MS- q ; i.e.,

$$\mathbf{p}_q \triangleq [\mathbf{p}_{q,1}^\dagger, \dots, \mathbf{p}_{q,M}^\dagger]^\dagger \in \mathbb{C}^{MN_t \times 1}. \quad (4)$$

We further assume SUD; i.e., each MS treats the interfering signals as noise, and that there is channel reciprocity (such as in time division duplex). Therefore, every S-RRH estimates the channels between it and each MS served by the cluster.

Assumption 3: The long term channel characteristics are locally known at each S-RRH and globally known at the CU; i.e., for each $m \in \mathcal{M}$, S-RRH- m knows $\{\alpha_{q,m}\}_{q \in \mathcal{Q}}$ whereas the CU knows $\{\alpha_{q,m}\}_{m \in \mathcal{M}, q \in \mathcal{Q}}$. Since these parameters are conveyed to the CU only once, the associated overhead on the Xn-link (cf. Fig. 1) is neglected. Moreover, for simplicity, we assume that each S-RRH- m , has perfect local CSI $\{\mathbf{h}_{q,m}\}_{q \in \mathcal{Q}}$; i.e., no estimation errors.

²We use the standard definition of a block-fading channel (see [27], Ch. 4.2); that is, a channel that remains constant during a certain time block, called the coherence time, which is much shorter than the code block length. This channel is drawn randomly at each coherence time, and forms an ergodic sequence over time.

Assumption 4: Since the Xn-link is rate limited, S-RRH- m quantizes its CSI and sends the indices of the quantization codewords $\{c_{q,m}\}_{q \in \mathcal{Q}}$ with an overall number of B bits to the CU. Upon receiving all the codewords $U = \{c_{q,m}\}_{q \in \mathcal{Q}, m \in \mathcal{M}}$, the CU estimates \mathbf{h}_q , $\forall q \in \mathcal{Q}$ as

$$\hat{\mathbf{h}}_q \triangleq [\hat{\mathbf{h}}_{q,1}^\dagger, \dots, \hat{\mathbf{h}}_{q,M}^\dagger]^\dagger \in \mathbb{C}^{MN_t \times 1} \quad (5)$$

where $\hat{\mathbf{h}}_{q,m}$ is the estimate of $\mathbf{h}_{q,m}$, $\forall q \in \mathcal{Q}$, $m \in \mathcal{M}$.

For now, we do not restrict ourselves to a particular quantization or estimation method. Henceforth, we refer to this procedure as the *standard* CSI feedback scheme. Based on $\{\hat{\mathbf{h}}_q\}_{q \in \mathcal{Q}}$, the CU calculates the overall joint precoding matrix as follows

$$\mathbf{p}_q \triangleq \mathbf{N}_q \frac{(\hat{\mathbf{h}}_q^\dagger \mathbf{N}_q)^\dagger}{\|\hat{\mathbf{h}}_q^\dagger \mathbf{N}_q\|}, \quad \forall q \in \mathcal{Q} \quad (6)$$

where the columns of $\mathbf{N}_q \in \mathbb{C}^{MN_t \times MN_t - (Q-1)}$ form an orthonormal basis for the null space of $\{\hat{\mathbf{h}}_j\}_{j \in \mathcal{Q}_{-q}}$. Henceforth, we refer to this scheme as ZF beamforming. After setting $\mathbf{p}_q, \forall q \in \mathcal{Q}$, the CU quantizes it and feeds each S-RRH with its corresponding components.

Assumption 5: For each m , the CU quantizes $\{\mathbf{p}_{q,m}\}_{q \in \mathcal{Q}}$ with overall B bits that are sent to S-RRH- m . The corresponding estimate at S-RRH- m , is denoted by $\{\hat{\mathbf{p}}_{q,m}\}_{q \in \mathcal{Q}}$.

Because \mathbf{p}_q is orthogonal to $\{\hat{\mathbf{h}}_j\}_{j \in \mathcal{Q}_{-q}}$ rather than $\{\mathbf{h}_j\}_{j \in \mathcal{Q}_{-q}}$, there is a performance loss with respect to the case of perfect CSI due to residual interference, even if $\hat{\mathbf{p}}_{q,m}$ is quantized without errors. For simplicity and analytical tractability, we assume that the data signals $s_q, q \in \mathcal{Q}$ are delivered to the S-RRHs without errors.

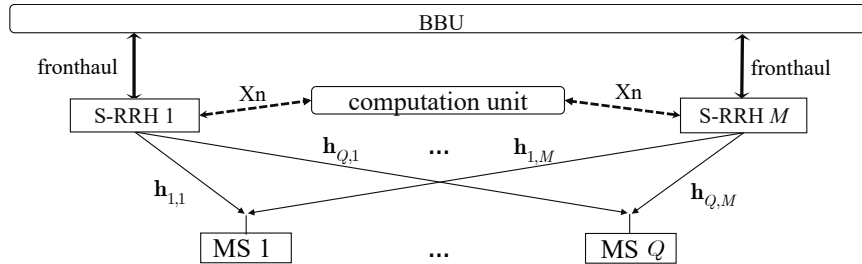


Fig. 1. System model. Due to low latency constraints, the CU is located close to the S-RRHs, and is interconnected via the low latency link, Xn; a link that may be separated from the fronthaul. It is, therefore, capable of carrying out real time operations, such as beamforming design. We assume that while the Xn-link is of low latency, it is rate-limited; a fact that decreases the CSI accuracy at the CU.

III. DOWNLINK CRAN-JT: PERFORMANCE ANALYSIS FOR ZF WITH IMPERFECT CSI

In this section, we introduce a new upper bound on the throughput degradation under limited CSI with respect to perfect CSI. For simplicity and analytical tractability, we assume that the channel magnitude information (CMI) $\|\mathbf{h}_{q,m}\|$, $\forall q \in \mathcal{Q}$, $m \in \mathcal{M}$ is perfectly conveyed to the CU, and that the channel directional information (CDI) $\bar{\mathbf{h}}_{q,m} \triangleq \mathbf{h}_{q,m}/\|\mathbf{h}_{q,m}\|$ is quantized separately using RVQ [25],³ with independent codebooks for every q, m . We make the same assumptions about $\{\mathbf{p}_{q,m}\}_{q \in \mathcal{Q}, m \in \mathcal{M}}$. We now review some of the properties of RVQ. Let $\hat{\mathbf{h}}_{q,m}$ be the output of RVQ with b bits. Then,

$$\bar{\mathbf{h}}_{q,m} = \sqrt{1 - Z_{q,m}} \hat{\mathbf{h}}_{q,m} + \sqrt{Z_{q,m}} \mathbf{s}_{q,m} \quad (7)$$

where $\mathbf{s}_{q,m}$ is a random vector uniformly distributed on the unit sphere of the null space of $\hat{\mathbf{h}}_{q,m}$, and $Z_{q,m}$ is a random variable, independent of $\mathbf{s}_{q,m}$, and distributed as the minimum of 2^b beta $(N_t - 1, 1)$ random variables [9]. Under the assumption of perfect CMI, the CU use

$$\hat{\mathbf{h}}_{q,m} = \|\mathbf{h}_{q,m}\| \hat{\mathbf{h}}_{q,m} , \quad (8)$$

as the estimate of $\mathbf{h}_{q,m}$.⁴ For analytical simplicity, we make the following assumption.

Assumption 6: Each S-RRH transmits with equal power to every MS; i.e., $P_q = P_{q,m} = P, \forall q \in \mathcal{Q}, m \in \mathcal{M}$ (cf. Assumption 2 for P_q).⁵ To prevent S-RRHs from violating their power constraint P_{\max} , we set $P = \frac{P_{\max}}{Q}$. Moreover, $n_q \sim \mathcal{CN}(0, 1)$ (cf. (3)).

From (3) and Assumption 6, the signal-to-interference-plus-noise ratio (SINR) at MS- q is

$$\text{SINR}_q(\{\hat{\mathbf{p}}_i\}_{i \in \mathcal{Q}}) \triangleq \frac{P|\mathbf{h}_q^\dagger \hat{\mathbf{p}}_q|^2}{1 + P \sum_{j \in \mathcal{Q} \setminus q} |\mathbf{h}_q^\dagger \hat{\mathbf{p}}_j|^2}, \quad \forall q \in \mathcal{Q} \quad (9)$$

where $\hat{\mathbf{p}}_q \triangleq [\hat{\mathbf{p}}_{q,1}^\dagger, \dots, \hat{\mathbf{p}}_{q,M}^\dagger]^\dagger \in \mathbb{C}^{MN_t \times 1}$, and $\hat{\mathbf{p}}_{q,m}$ is the estimate of $\mathbf{p}_{q,m}$ under RVQ, similar to (8). Assuming a Gaussian codebook, and SUD, the achievable ergodic rate of MS- q with imperfect CSI is

$$\hat{R}_q \triangleq \mathbb{E}\{\log(1 + \text{SINR}_q(\{\hat{\mathbf{p}}_i\}_{i \in \mathcal{Q}}))\} \quad (10)$$

³In RVQ, the codebook is generated randomly from a uniform distribution over the unit sphere.

⁴Note that $\mathbb{E}\{\mathbf{h}_{q,m} \|\mathbf{h}_{q,m}\|, \hat{\mathbf{h}}_{q,m}\}$, the minimum mean square error estimate of $\mathbf{h}_{q,m}$, is given by $\mathbb{E}\{\sqrt{1 - Z_{q,m}}\} \|\mathbf{h}_{q,m}\| \hat{\mathbf{h}}_{q,m}$. Since this paper considers only ZF-type strategies, the factor $\mathbb{E}\{\sqrt{1 - Z_{q,m}}\}$ does not affect the beamformer, and therefore, omitted.

⁵Note that the equal power assumption is not optimal (see e.g. [29]) and was made to simplify the analysis, which is already very complicated.

The expectation is taken with respect to the joint distribution of the channel and the RVQ's random codebook.⁶ To evaluate performance, later we will compare \hat{R}_q to the corresponding throughput R_q^* without quantization error; i.e.,

$$R_q^* \stackrel{\Delta}{=} \mathbb{E}\{\log(1 + \text{SINR}_q(\{\mathbf{p}_i^*\}_{i \in \mathcal{Q}}))\} \quad (11)$$

where \mathbf{p}_q^* is given in (6) while substituting $\hat{\mathbf{h}}_q = \mathbf{h}_q, \forall q \in \mathcal{Q}$, and is assumed to be fed-back perfectly.

Theorem 1: Consider Assumptions 1 and 3 to 6 and define the rate loss as

$$\Delta R_q \stackrel{\Delta}{=} R_q^* - \hat{R}_q \quad (12)$$

where \hat{R}_q and R_q^* are defined in (10) and (11), respectively. Consider some $q \in \mathcal{Q}$ and without loss of generality assume that $\alpha_q = 1$, where $\alpha_q \stackrel{\Delta}{=} \sum_{m=1}^M \alpha_{q,m}$. Assuming that $\mathbf{h}_{q',m}, \mathbf{p}_{q',m}$ are quantized with $B/Q \in \mathbb{N}$ bits (cf. Assumptions 4 and 5), each, $\forall q' \in \mathcal{Q}, \forall m \in \mathcal{M}$; then

$$\Delta R_q \leq \Delta \bar{R}_{1,q} + \Delta \bar{R}_{2,q} \quad (13)$$

where

$$\begin{aligned} \Delta \bar{R}_{1,q} &\stackrel{\Delta}{=} \log \left\{ 1 + \frac{PN_t(Q-1)}{M} \times \left[\frac{1}{N_t-1} 2^{\frac{-B}{Q(N_t-1)}} \left(2(1 - \mathcal{U}(2^{B/Q}, a)) + 2^{\frac{-B}{Q(N_t-1)}} \right) \right. \right. \\ &\quad \left. \left. + (1 - \mathcal{U}(2^{B/Q}, a))^2 - (1 - \mathcal{U}(2^{B/Q}, a)/2 - \mathcal{U}(2^{B/Q}, 2a))^4 \right] \right\} \end{aligned} \quad (14)$$

$$\begin{aligned} \Delta \bar{R}_{2,q} &\stackrel{\Delta}{=} 6R_q^* (\mathcal{U}(2^{B/Q}, a) + \mathcal{V}_M(2^{B/Q}, a)) \\ &\quad + \frac{\pi \sqrt{P} N_t M}{\sqrt{2}} U\left(\frac{1}{2}, \frac{1-N_t M}{2}, \frac{1}{2P}\right) (\mathcal{U}(2^{B/Q}, a/2) + \mathcal{V}_M(2^{B/Q}, a/2)) \end{aligned} \quad (15)$$

Here $a = \frac{1}{N_t-1}$, $P = \frac{P_{\max}}{Q}$, $U(\cdot)$ is confluent hypergeometric function and⁷

$$\mathcal{U}(x, a) = x\beta(x, 1+a) \quad (16)$$

$$\mathcal{V}_M(x, a) = \frac{(M-1)}{\sqrt{2M-1}} \sqrt{\mathcal{U}(x, 2a) - \mathcal{U}(x, a)^2} \quad (17)$$

where $\beta(\cdot)$ is the Beta function.

Remark 1: Under Assumption 1, the perfect-CSI rate, R_q^* , can be calculated based on known results. For example, consider the case where the long-term channel-attenuation is equal for each

⁶Note that \mathbf{p}_i is a function of the quantization $\hat{\mathbf{h}}_q$, which, in the case of RVQ, is a function of the channels $\{\mathbf{h}_{q,m}\}_{m \in \mathcal{M}}$ and of the codebook generated for each channel. Moreover, $\hat{\mathbf{p}}_i$ is a function of $\{\mathbf{p}_{i,m}\}_{m \in \mathcal{M}}$.

⁷Note that $\mathbb{E}\{Z_{q,m}^i\} = \mathcal{U}(2^{B/Q}, ai)$, where $Z_{q,m}$ is defined in (7).

S-RRH; i.e., $\alpha_{q,m} = \alpha_{q,m'} \forall m, m' \in \mathcal{M}$, and without loss of generality, assume that $\alpha_{q,m} = 1/M \forall m \in \mathcal{M}$. In this case, it is straightforward to show (see Supplementary A) that

$$R_q^* = R^* = \mathbb{E}\{\log(1 + P|\mathbf{h}_q^\dagger \mathbf{p}_q^*|^2)\} = (\log e)e^{\frac{M}{P}} \sum_{k=0}^{T-1} \Gamma\left(-k, \frac{M}{P}\right) \left(\frac{M}{P}\right)^k \triangleq \varphi(T, P/M) \quad (18)$$

where, $T = MN_t - (Q - 1)$ and $\Gamma(\cdot, \cdot)$ is the incomplete Gamma function. In the case where $\exists m \neq m'$ such that $\alpha_{q,m} \neq \alpha_{q,m'}$, obtaining an expression similar to (18) is complicated even for the two-S-RRH case (see [30]). Nevertheless, R_q^* can be approximated; see [30] Sec IV.A for the two-S-RRH case and [31, 32] for more than two-S-RRHs.

Proof of Theorem 1: By the assumptions of Theorem 1 and using (9), (10), (11) and (12) it follows that

$$\begin{aligned} \Delta R_q = & \mathbb{E}\{\log(1 + P|\mathbf{h}_q^\dagger \mathbf{p}_q^*|^2)\} - \mathbb{E}\left\{\log\left(1 + P|\mathbf{h}_q^\dagger \hat{\mathbf{p}}_q|^2 + P \sum_{j \in \mathcal{Q}_{-q}} |\mathbf{h}_q^\dagger \hat{\mathbf{p}}_j|^2\right)\right\} \\ & + \mathbb{E}\left\{\log\left(1 + P \sum_{j \in \mathcal{Q}_{-q}} |\mathbf{h}_q^\dagger \hat{\mathbf{p}}_j|^2\right)\right\} \leq A_1 - A_2 + A_3 \end{aligned} \quad (19)$$

where $\hat{\mathbf{p}}_q$ and \mathbf{p}_q^* are defined in (9) and (11), respectively, and $A_1 = \mathbb{E}\{\log(1 + P|\mathbf{h}_q^\dagger \mathbf{p}_q^*|^2)\}$, $A_2 = \mathbb{E}\{\log(1 + P|\mathbf{h}_q^\dagger \hat{\mathbf{p}}_q|^2)\}$, $A_3 = \mathbb{E}\{\log(1 + P \sum_{j \in \mathcal{Q}_{-q}} |\mathbf{h}_q^\dagger \hat{\mathbf{p}}_j|^2)\}$. The inequality (19) follows because $P \sum_{j \in \mathcal{Q}_{-q}} |\mathbf{h}_q^\dagger \hat{\mathbf{p}}_j|^2 \geq 0$ and $\log(\cdot)$ is a monotone increasing function. The desired result (13) then follows from the following lemmas.

Lemma 2: Under the assumptions of Theorem 1, $A_3 \leq \Delta \bar{R}_{1,q}$ (cf. (19), (14)). ■

Proof: See Appendix A. ■

Lemma 3: Under the assumptions of Theorem 1, $A_1 - A_2 \leq \Delta \bar{R}_{2,q}$ (cf. (19), (15)). ■

Proof: See Appendix C. ■

Substituting Lemmas 2 and 3 into (19), establishes (13). ■

The bound in Theorem 1 can be further simplified using a lower order approximation as follows.

Corollary 4: The bound $\Delta R_q \leq \Delta \bar{R}_{1,q} + \Delta \bar{R}_{2,q}$ in (13) can be further approximated as

$$\begin{aligned} \Delta \bar{R}_{1,q} + \Delta \bar{R}_{2,q} &= 2^{\frac{-B}{2Q(N_t-1)}} \frac{\pi \sqrt{P} N_t M}{\sqrt{2}} U\left(\frac{1}{2}, \frac{1 - N_t M}{2}, \frac{1}{2P}\right) \\ &\quad \times \left[V_M\left(\frac{1/2}{N_t-1}\right) + \Gamma\left(\frac{1/2}{N_t-1} + 1\right) \right] + O(2^{\frac{-B}{Q(N_t-1)}}) \end{aligned} \quad (20)$$

where $\Gamma(\cdot)$ is the Gamma function and $V_M(a) = \sqrt{\Gamma(2a+1) - \Gamma(a+1)^2} (M-1) / \sqrt{2M-1}$.

Proof: Let $z = 2^{B/Q}$ and denote

$$\Delta\bar{R}_{1,q}(z) + \Delta\bar{R}_{2,q}(z) = \log(1 + W_1(z) + W_2(z)) + W_3(z) \quad (21)$$

where $\Delta\bar{R}_{1,q}$ and $\Delta\bar{R}_{2,q}$ are defined in (14) and (15), respectively, and $W_1(z) = P(Q-1)z^{-a}N_t(2(1-\mathcal{U}(z,a))+z^{-a})/M(N_t-1)$, $W_2(z) = P(Q-1)N_t/M[(1-\mathcal{U}(z,a))^2 - (1-\mathcal{U}(z,a)/2 - \mathcal{U}(z,2a))^4]$, $W_3(z) = \pi\sqrt{P}N_tM[\mathcal{U}(z,a/2) + \mathcal{V}_M(z,a/2)]U(\frac{1}{2}, \frac{1-N_tM}{2}, \frac{1}{2P})/\sqrt{2} + 6R_q^* \times [\mathcal{U}(z,a) + \mathcal{V}_M(z,a)]$. It can be shown that

$$\mathcal{U}(z,a) = \Gamma(a+1)z^{-a} + O(z^{-a-\frac{1}{2}}). \quad (22)$$

By substituting the latter into $W_1(z)$, it can be shown that $W_1(z) = \frac{2P(Q-1)z^{-a}N_t}{M(N_t-1)} + O(z^{-2a})$. Now to $W_2(z)$. Substituting, (22), it can be shown that $W_2(z) = P(Q-1)N_t/M[(1-\Gamma(a+1)z^{-a})^2 - (1-\Gamma(a+1)z^{-a}/2)^4]$. Moreover, because $(1-x)^2 - (1-x/2)^4 = -\frac{x^4}{16} + \frac{x^3}{2} - \frac{x^2}{2}$, it follows that $W_2(z) = O(z^{-2a})$. Finally we turn to, $W_3(z)$. Because $\mathcal{U}(z,a) + \mathcal{V}_M(z,a) = (V_M(z,a) + \Gamma(a+1))z^{-a} + O(z^{-a-1})$, it follows that $W_3(z) = \frac{\pi\sqrt{P}N_tM}{\sqrt{2}}U(\frac{1}{2}, \frac{1-N_tM}{2}, \frac{1}{2P})z^{-\frac{a}{2}}[V_M(a/2) + \Gamma(1+a/2)] + 6R_q^*z^{-a}[V_M(a) + \Gamma(a+1)] + O(z^{-1-\frac{a}{2}})$. Then, by substituting W_1 , W_2 and W_3 into (21) while taking lower order terms, the desired result follows. ■

We conclude this section with some insights. From Corollary 4 it follows that the rate-gap decreases like $2^{\frac{-B}{2Q(N_t-1)}}$ as B increases. Furthermore, note that $U(1/2, (1-N_tM)/2, 1/(2P)) = O(1)$ as $P \rightarrow \infty$. Therefore, to maintain the overall number of degrees of freedom, $2^{\frac{-B}{2Q(N_t-1)}}$ should decrease at least like \sqrt{P} ; i.e., the number of bits per channel should, at least, increase linearly with the signal-to-noise ratio (SNR) in dB as well as with the number of MSs. Otherwise, the network is interference limited. This result is consistent with previous findings on the single-Tx broadcast channel (cf. [9]). Finally, the rate gap decrease of $2^{\frac{-B}{2Q(N_t-1)}}$ implies that it is possible to reduce the rate gap without increasing B , by having a smaller Q , or by having an effective number of antennas that is less than N_t . The latter insight is the motivation for the P&Q CSI sharing scheme presented in the following section.

Note, however, that while ΔR_q is improved if N_t or Q decreases, R_q^* is deteriorating due to a loss in antenna gain. This trade-off determines if the achievable-rate, \hat{R}_q (cf. (12)), increases or decreases. In the sequel, we show that \hat{R}_q can be drastically improved under a good precoding strategy in most cases. Numerical results for the proposed bounds are given in Sec. VI.

IV. THE PRECODE AND QUANTIZE CSI SHARING SCHEME

The P&Q CSI sharing scheme aims at reducing CSI overhead in the Xn-link as well as the fronthaul information rate. Each S-RRH, say S-RRH- m , applies a front-end precoding matrix $\mathbf{A}_m \in \mathbb{C}^{N_t \times \tilde{N}_t}$, calculated according to its local CSI $\{\mathbf{h}_{q,m}\}_{q \in \mathcal{Q}}$. This creates effective low-dimensional channels $\tilde{\mathbf{h}}_{q,m}^\dagger = \mathbf{h}_{q,m}^\dagger \mathbf{A}_m \in \mathbb{C}^{1 \times \tilde{N}_t}$, $\forall q \in \mathcal{Q}$, with $\tilde{N}_t < N_t$, which can be quantized more accurately than $\mathbf{h}_{q,m}$ [11]. We further denote the overall effective channel as $\tilde{\mathbf{h}}_q \triangleq [\tilde{\mathbf{h}}_{q,1}^\dagger, \dots, \tilde{\mathbf{h}}_{q,M}^\dagger]^\dagger \in \mathbb{C}^{M\tilde{N}_t \times 1}$.

Definition 1 (MS allocation policy): To determine \mathbf{A}_m , S-RRH- m picks a subset of the MSs $\bar{\mathcal{S}}_m \subset \mathcal{Q}$, where $|\bar{\mathcal{S}}_m| = \bar{Q}$, according to the policy detailed next. Knowing $\{\alpha_{q,m}\}_{q \in \mathcal{Q}}$ S-RRH- m , picks \bar{Q} MSs that have the largest attenuation factor; that is, $\bar{\mathcal{S}}_m$ includes MSs such that $\alpha_{q,m} \leq \alpha_{q',m}$, $\forall q \in \bar{\mathcal{S}}_m$, $q' \in \mathcal{Q} \setminus \bar{\mathcal{S}}_m$.

Given $\bar{\mathcal{S}}_m$, \mathbf{A}_m is set as the projection matrix into the null space of the matrix whose columns are given by $\{\mathbf{h}_{q,m}\}_{q \in \bar{\mathcal{S}}_m}$; i.e.,

$$\mathbf{A}_m = [\mathbf{u}_1 \cdots \mathbf{u}_{\tilde{N}_t}], \quad \mathbf{u}_i \in \mathbb{C}^{N_t \times 1} \quad (23)$$

where $\tilde{N}_t = N_t - \bar{Q}$ and $\{\mathbf{u}_i\}_{i=1}^{\tilde{N}_t}$ is an orthonormal basis for the orthogonal complement of $\text{span}(\{\mathbf{h}_{q,m}\}_{q \in \bar{\mathcal{S}}_m})$. Thus, S-RRH- m now serves only $Q - \bar{Q}$ MSs, which we denote by $\mathcal{S}_m = \mathcal{Q} \setminus \bar{\mathcal{S}}_m \subset \mathcal{Q}$.⁸ From (23), and because each S-RRH has perfect local CSI, $\tilde{\mathbf{h}}_{q,m} = \mathbf{0}_{\tilde{N}_t}$, $\forall q \in \bar{\mathcal{S}}_m$. Thus, S-RRH- m now sends the CU only $Q - \bar{Q}$ channels $\{\tilde{\mathbf{h}}_{q,m}\}_{q \in \mathcal{S}_m}$, of lower dimension $\tilde{N}_t < N_t$, which can be quantized more accurately. Denote the estimate of $\tilde{\mathbf{h}}_{q,m}$ at the CU by $\hat{\tilde{\mathbf{h}}}_{q,m}$ and

$$\hat{\tilde{\mathbf{h}}}_q \triangleq [\hat{\tilde{\mathbf{h}}}_{q,1}^\dagger, \dots, \hat{\tilde{\mathbf{h}}}_{q,M}^\dagger]^\dagger \in \mathbb{C}^{M\tilde{N}_t \times 1}. \quad (24)$$

Since the CU knows $\bar{\mathcal{S}}_m$ ⁹ it also knows that $\tilde{\mathbf{h}}_{q,m} = \mathbf{0}_{\tilde{N}_t}$, $\forall q \in \bar{\mathcal{S}}_m, m \in \mathcal{M}$. Thus, only $\{\tilde{\mathbf{h}}_{q,m}\}_{q \in \mathcal{S}_m, m \in \mathcal{M}}$ are estimated by it, whereas $\{\hat{\tilde{\mathbf{h}}}_{q,m}\}_{q \in \bar{\mathcal{S}}_m, m \in \mathcal{M}}$ are set to zero; i.e., $\hat{\tilde{\mathbf{h}}}_{q,m} = \mathbf{0}_{\tilde{N}_t}$, $\forall m \in \mathcal{M}, q \in \bar{\mathcal{S}}_m$. Upon receiving the CSI from all S-RRHs, $\{\tilde{\mathbf{h}}_q\}_{q \in \mathcal{Q}}$, the CU computes $\{\tilde{\mathbf{p}}_q\}_{q \in \mathcal{Q}}$, where

$$\tilde{\mathbf{p}}_q \triangleq [\tilde{\mathbf{p}}_{q,1}^\dagger, \dots, \tilde{\mathbf{p}}_{q,M}^\dagger]^\dagger \in \mathbb{C}^{M\tilde{N}_t \times 1} \quad (25)$$

⁸Under this policy, MSs may remain unserved; i.e., $q \in \bar{\mathcal{S}}_m, \forall m \in \mathcal{M}$. In this case, these MSs can be reallocated at the expense of MSs that are served by the largest number of S-RRHs.

⁹Because the CU knows $\{\alpha_{q,m}\}_{m \in \mathcal{M}, q \in \mathcal{Q}}$ (cf. Assumption 3), it can determine $\bar{\mathcal{S}}_m$ by applying the policy given in Definition 1, and therefore also knows \tilde{N}_t .

is the overall beamformer designated for MS- q .

Remark 2: Since each S-RRH only serves a subset of the MSs, full data sharing is unnecessary. Note that $\tilde{\mathbf{h}}_q$ satisfies $\tilde{\mathbf{h}}_q = \tilde{\mathbf{h}}_q \odot (\mathbf{v}_q \otimes \mathbf{1}_{\tilde{N}_t})$, where \mathbf{v}_q is an M dimensional vector satisfying $[\mathbf{v}_q]_m = 1$ if S-RRH- m serves MS- q , and 0 otherwise.¹⁰ Therefore, if $\tilde{\mathbf{p}}_q \neq \tilde{\mathbf{p}}_q \odot (\mathbf{v}_q \otimes \mathbf{1}_{\tilde{N}_t})$, it follows that some S-RRHs, which do not serve MS- q , do transmit s_q . Explicitly, if $\tilde{\mathbf{h}}_{q,m} = \mathbf{0}_{\tilde{N}_t}$ and $\tilde{\mathbf{p}}_{q,m} \neq \mathbf{0}_{\tilde{N}_t}$ for some $m \in \mathcal{M}$, S-RRH- m must transmit the signal s_q , which is not received by MS- q . To avoid transmitting more data than necessary, we set the beamformer $\tilde{\mathbf{p}}_q$ orthogonal to $\{\hat{\mathbf{h}}_j \odot (\mathbf{v}_q \otimes \mathbf{1}_{\tilde{N}_t})\}_{j \in \mathcal{Q}_{-q}}$ from which it follows that $\tilde{\mathbf{p}}_q = \tilde{\mathbf{p}}_q \odot (\mathbf{v}_q \otimes \mathbf{1}_{\tilde{N}_t})$; i.e., the beamformer's weights corresponding to S-RRHs that do not serve MS- q are zero. By not sending $\{s_q\}_{q \in \mathcal{S}_m}$ to S-RRH- m , we reduce the number of data streams to that S-RRH to $Q - \bar{Q}$, rather than Q as in the standard scheme.

Definition 2: The beamformer for MS- q in the P&Q scheme is given by $\tilde{\mathbf{p}}_q \triangleq \tilde{\mathbf{N}}_q \frac{(\hat{\mathbf{h}}_q^\dagger \tilde{\mathbf{N}}_q)^\dagger}{\|\hat{\mathbf{h}}_q^\dagger \tilde{\mathbf{N}}_q\|}$, $\forall q \in \mathcal{Q}$, and dubbed P&Q beamformer. Here, $\tilde{\mathbf{N}}_q \in \mathbb{C}^{M\tilde{N}_t \times M\tilde{N}_t - (\tilde{Q}_q - 1)}$ is the projection matrix into the null space of $\{\hat{\mathbf{h}}_j \odot (\mathbf{v}_q \otimes \mathbf{1}_{\tilde{N}_t})\}_{j \in \mathcal{Q}_{-q}}$. The factor \tilde{Q}_q is the number of MSs such that $\hat{\mathbf{h}}_q^\dagger \hat{\mathbf{h}}_j \neq 0$, $\forall q, j \in \mathcal{Q}$; i.e., $\tilde{Q}_q = Q - \sum_{j \in \mathcal{Q}_{-q}} \chi_{\{0\}}(M_{q,j})$, where $M_{q,j}$ is the number of S-RRHs that serve both MS- q and MS- j .

Remark 3: The coefficient \tilde{Q}_q (cf. Definition 2) is, in fact, the number of MSs served by at least one of the S-RRHs that serve MS- q . $\tilde{Q}_q - 1$ is the number of MSs to which the interference inflicted by MS- q signal must be zeroed by the ZF precoder.

After setting $\tilde{\mathbf{p}}_q$ according to Definition 2, the CU quantizes $\tilde{\mathbf{p}}_{q,m}$, (cf. (25)) and sends each S-RRH its relevant precoders. Moreover, because $\{\tilde{\mathbf{p}}_{q,m}\}_{q \in \mathcal{S}_m, m \in \mathcal{M}} = \mathbf{0}_{\tilde{N}_t}$, the CU does not have to send S-RRH- m the entire set $\{\tilde{\mathbf{p}}_{q,m}\}_{q \in \mathcal{Q}}$, but rather sends $\{\tilde{\mathbf{p}}_{q,m}\}_{q \in \mathcal{S}_m}$, which consists solely of $Q - \bar{Q}$ beamformers. In more explicit terms, it sends the quantization of $\{\tilde{\mathbf{p}}_{q,m}\}_{q \in \mathcal{S}_m}$ to S-RRH- m . Since the latter have a lower dimension $\tilde{N}_t < N_t$, they can be quantized more accurately. Once having received these quantization, S-RRH- m sets its overall beamformer toward MS- q as

$$\hat{\mathbf{p}}_{q,m}^{\text{P&Q}} \triangleq \mathbf{A}_m \hat{\mathbf{p}}_{q,m} \in \mathbb{C}^{N_t \times 1} \quad (26)$$

where $\hat{\mathbf{p}}_{q,m}$ denotes the estimate of $\tilde{\mathbf{p}}_{q,m}$.

¹⁰In the standard scheme, where every S-RRH serves every MS, $\mathbf{v}_q = \mathbf{1}_M$, $\forall q \in \mathcal{Q}$.

Definition 3: The overall beamformer $\hat{\mathbf{p}}_q^{\text{P\&Q}} \in \mathbb{C}^{MN_t} \times 1$ for MS- q in the P&Q scheme is given by $\hat{\mathbf{p}}_q^{\text{P\&Q}} \triangleq \mathbf{A}\hat{\mathbf{p}}_q$, where $\mathbf{A} = \text{blockdiag}\{\mathbf{A}_1, \mathbf{A}_2, \dots, \mathbf{A}_M\} \in \mathbb{C}^{MN_t \times M\tilde{N}_t}$ and $\hat{\mathbf{p}}_q \in \mathbb{C}^{M\tilde{N}_t \times 1}$ is given by $\hat{\mathbf{p}}_q \triangleq [\hat{\mathbf{p}}_{q,1}^\dagger, \dots, \hat{\mathbf{p}}_{q,M}^\dagger]^\dagger \in \mathbb{C}^{M\tilde{N}_t \times 1}$.

Note that because $\tilde{\mathbf{p}}_q = \tilde{\mathbf{p}}_q \odot (\mathbf{v}_q \otimes \mathbf{1}_{\tilde{N}_t})$ it follows that $\hat{\mathbf{p}}_q = \hat{\mathbf{p}}_q \odot (\mathbf{v}_q \otimes \mathbf{1}_{\tilde{N}_t})$.

Definition 4: Let \mathcal{M}_q be the set of S-RRHs that serve MS- q ; that is, $\mathcal{M}_q = \{m \in \mathcal{M} : q \in \mathcal{S}_m\}$ and denote $M_q = |\mathcal{M}_q|$. Furthermore, let $\mathcal{M}_{q,j} \triangleq \mathcal{M}_q \cap \mathcal{M}_j$ be the set of S-RRHs that serve both MS- q and MS- j , and denote $M_{q,j} = |\mathcal{M}_{q,j}|$.

Substituting $\hat{\mathbf{p}}_i^{\text{P\&Q}}$ for $\mathbf{p}_i, i \in \mathcal{Q}$ in (3), MS- q observes the signal

$$y_q = \tilde{\mathbf{h}}_q^\dagger \hat{\mathbf{p}}_q s_q + \sum_{j \in \mathcal{Q}_q} \tilde{\mathbf{h}}_q^\dagger \hat{\mathbf{p}}_j s_j + n_q, \quad \forall q \in \mathcal{Q} \quad (27)$$

where $\tilde{\mathbf{h}}_q = [\tilde{\mathbf{h}}_{q,1}^\dagger, \dots, \tilde{\mathbf{h}}_{q,M}^\dagger]^\dagger$ and $\hat{\mathbf{p}}_q$ is given in Definition 3. The latter can be written as

$$y_q = \sum_{m \in \mathcal{M}_q} \tilde{\mathbf{h}}_{q,m}^\dagger \hat{\mathbf{p}}_{q,m} s_q + \sum_{j \in \mathcal{Q}_q} \sum_{m \in \mathcal{M}_{q,j}} \tilde{\mathbf{h}}_{q,m}^\dagger \hat{\mathbf{p}}_{j,m} s_j + n_q \quad (28)$$

where \mathcal{M}_q and $\mathcal{M}_{q,j}$ are given in Definition 4.

The advantage of the proposed scheme is twofold. From [9], it is known that when quantizing an N -dimensional uncorrelated Rayleigh fading channel with b bits, the quantization error is bounded above by $2^{-\frac{b}{N-1}}$. Therefore, the P&Q has a smaller CSI-quantization error because the channels and beamformers are $(\tilde{N}_t - 1)$ -dimensional, rather than $(N_t - 1)$. Furthermore, since each S-RRH serves fewer MSs, fewer channels and beamformers are delivered to the CU and S-RRHs, respectively, through the limited-rate links. Assuming an overall budget of B bits for each S-RRH, in the P&Q scheme each channel is allocated $B/(Q - \bar{Q})$ bits rather than B/Q as in the standard scheme. Consequently, the quantization error is bounded by $2^{-\frac{B}{(Q - \bar{Q})(\tilde{N}_t - 1)}}$ rather than by $2^{-\frac{B}{Q(N_t - 1)}}$. The second advantage of P&Q scheme is in reducing fronthaul data load, which is a major problem in C-RAN. This follows from the fact that each S-RRH serves only $Q - \bar{Q}$ MSs. Hence, fewer data signals must be transferred via the fronthaul between the BBU to each S-RRH. Moreover, because each S-RRH now serves fewer MSs, the overall power allocated for each MS may be increased.

V. THE P&Q SCHEME: PERFORMANCE ANALYSIS

We now present results corresponding to Theorem 1 and Corollary 4, for the P&Q scheme. The analysis is based on the following assumptions.

Assumption 7: Each S-RRH serves $Q - \bar{Q}$ MSs, with $\tilde{P}_{q,m} = \tilde{P} = \frac{P_{\max}}{Q - \bar{Q}}$, $\forall q \in \mathcal{Q}$, $m \in \mathcal{M}$.

Because the analysis of the P&Q is more complicated than the standard scheme, we simplify the setup as follow.

Assumption 8 (symmetric system-geometry with an equal pathloss constrain): The long term channel attenuation satisfies $\alpha_{q,m} = 1/M$, $\forall q \in \mathcal{Q}$, $m \in \mathcal{M}$.

This assumption is applicable if, for example, S-RRHs are placed on the edges of a regular polygon with M nodes and MSs are placed close to each other at the center of that polygon.¹¹ Then, MSs have approximately the same long term channel attenuation to each S-RRH. In a rich scattering environment, the MSs will experience independent fading.¹²

Definition 5: Consider Assumptions 7 and 8, let $\Delta \tilde{R}_q \triangleq R_q^* - \hat{\tilde{R}}_q$ be the P&Q rate-gap where R_q^* is given in (11), $\hat{\tilde{R}}_q = \mathbb{E}\{\log(1 + \text{SINR}_q(\{\hat{\mathbf{p}}_i^{\text{P\&Q}}\}_{i \in \mathcal{Q}}))\}$, and $\text{SINR}_q(\cdot)$ is defined similarly to (9) with $\hat{\mathbf{p}}_i^{\text{P\&Q}}$ as its argument (cf. Definition 3) while substituting \tilde{P} for P .

Definition 6: Let $\tilde{\mathbf{p}}_q^*$ be the P&Q beamformer without quantization error; i.e., $\tilde{\mathbf{p}}_q^*$ is obtained by replacing $\hat{\tilde{\mathbf{h}}}_q$ with $\tilde{\mathbf{h}}_q$ in $\tilde{\mathbf{p}}_q$ (cf. Definition 2) as well as in the calculation of $\tilde{\mathbf{N}}_q$. We further denote the P&Q inherent rate-loss by $\Delta R_{\text{AG},q} \triangleq R_q^* - \tilde{R}_q^*$ where R_q^* is given in (11) and $\tilde{R}_q^* = \mathbb{E}\{\log(1 + \tilde{P}|\tilde{\mathbf{h}}_q^\dagger \tilde{\mathbf{p}}_q^*|^2)\}$. In other words, $\Delta R_{\text{AG},q}$ is the difference between the rates of the standard scheme and P&Q scheme without quantization errors, which is a result of the loss in array-gain.

Theorem 5: Consider Assumptions 1, 3 to 5, 7 and 8, and assume that the P&Q (cf. Definition 2) is applied with B bits, (cf. Assumptions 4 and 5), where $\tilde{\mathbf{h}}_{q',m}$ and $\tilde{\mathbf{p}}_{q',m}$ are quantized using RVQ with $B/(Q - \bar{Q})$ (assumed integer) bits $\forall q' \in \mathcal{Q}$, $\forall m \in \mathcal{M}$. Then, the MS- q , $q \in \mathcal{Q}$ expected throughput-loss due to CSI quantization, in comparison to a perfect CSI satisfies

$$\Delta \tilde{R}_q \leq \Delta \tilde{R}_{1,q} + \Delta \tilde{R}_{2,q} + \Delta R_{\text{AG},q} \quad (29)$$

¹¹In more explicit terms, S-RRHs are placed at $\mathcal{G} = \{(r \cos(2\pi m/M), r \sin(2\pi m/M)) \in \mathbb{R}^2 : m \in \{0, \dots, M-1\}\}$, where $r > 0$ is fixed where $(0, 0)$ is the center of the polygon. The MSs are placed very close to each other around the point $(0, 0)$.

¹²This happens as long as the distance between them is larger than the wavelength; which is a very reasonable since cellular wavelengths are typically on the order of centimeters.

where

$$\begin{aligned} \Delta \tilde{R}_{1,q} &\stackrel{\Delta}{=} \log \left\{ 1 + \tilde{P} \left[\sum_{j \in \mathcal{Q}_{-q}} \frac{\tilde{N}_t M_{q,j}}{M_j M} \right] \times \left[\frac{1}{\tilde{N}_t - 1} 2^{\frac{-B}{(Q-Q)(\tilde{N}_t-1)}} \left(2(1 - \mathcal{U}(2^{\frac{B}{Q-Q}}, \tilde{a})) + 2^{\frac{-B}{(Q-Q)(\tilde{N}_t-1)}} \right) \right. \right. \\ &\quad \left. \left. + (1 - \mathcal{U}(2^{\frac{B}{Q-Q}}, \tilde{a}))^2 - (1 - \mathcal{U}(2^{\frac{B}{Q-Q}}, \tilde{a})/2 - \mathcal{U}(2^{\frac{B}{Q-Q}}, 2\tilde{a}))^4 \right] \right\} \end{aligned} \quad (30)$$

$$\begin{aligned} \Delta \tilde{R}_{2,q} &\stackrel{\Delta}{=} 6\tilde{R}_q^* (\mathcal{U}(2^{\frac{B}{Q-Q}}, \tilde{a}) + \mathcal{V}_{M_q}(2^{\frac{B}{Q-Q}}, \tilde{a})) \\ &\quad + \frac{\pi \sqrt{\tilde{P} \tilde{N}_t M_q}}{\sqrt{2}} U\left(\frac{1}{2}, \frac{1 - \tilde{N}_t M_q}{2}, \frac{1}{2\tilde{P}}\right) (\mathcal{U}(2^{\frac{B}{Q-Q}}, \tilde{a}/2) + \mathcal{V}_{M_q}(2^{\frac{B}{Q-Q}}, \tilde{a}/2)) \end{aligned} \quad (31)$$

Here, $\tilde{a} = \frac{1}{\tilde{N}_t - 1}$, $\tilde{P} = \frac{P_{\max}}{Q-Q}$, $M_q, M_{q,j}$ are defined in Definition 4 and $\mathcal{U}(\cdot), \mathcal{V}_M(\cdot)$ are defined in Theorem 1. Furthermore, the term $\Delta R_{\text{AG},q}$ (cf. (29) as well as Definition 6) satisfies

$$\Delta R_{\text{AG},q} = \varphi(T, P/M) - \varphi(\tilde{T}_q, \tilde{P}/M) \quad (32)$$

where $\varphi(\cdot)$ and T are defined in (18), $\tilde{T}_q = M_q \tilde{N}_t - (\tilde{Q}_q - 1)$, and \tilde{Q}_q is defined in Definition 2.

Proof: Similar to (19) it can be shown that

$$\Delta \tilde{R}_q \leq \tilde{A}_1 + \Delta R_{\text{AG},q} - \tilde{A}_2 + \tilde{A}_3 \quad (33)$$

where $\tilde{A}_1 = \mathbb{E}\{\log(1 + \tilde{P}|\tilde{\mathbf{h}}_q^\dagger \tilde{\mathbf{p}}_q^*|^2)\}$, $\tilde{A}_2 = \mathbb{E}\{\log(1 + \tilde{P}|\tilde{\mathbf{h}}_q^\dagger \hat{\mathbf{p}}_q|^2)\}$, $\tilde{A}_3 = \mathbb{E}\{\log(1 + \tilde{P} \sum_{j \in \mathcal{Q}_{-q}} |\tilde{\mathbf{h}}_q^\dagger \hat{\mathbf{p}}_j|^2)\}$ and the extra term is given by $\Delta R_{\text{AG},q} = A_1 - \tilde{A}_1$ where A_1 is defined in (19). The proof then follows from the following lemmas.

Lemma 6: Under the assumptions of Theorem 5, $\tilde{A}_3 \leq \Delta \tilde{R}_{1,q}$ (cf. (33), (30)).

Proof: See Appendix B. ■

Lemma 7: Under the assumptions of Theorem 5, $\tilde{A}_1 - \tilde{A}_2 \leq \Delta \tilde{R}_{2,q}$ (cf. (33), (31)).

Proof: See Appendix D. ■

After substituting the inequalities of Lemmas 6 and 7 into (33) it remains to show (32). To this end, we use $R^* = \varphi(T, P/M)$ (cf. (18)) and $\tilde{A}_1 = \varphi(\tilde{T}_q, \tilde{P}/M)$, which is obtained by applying the former while replacing T and P with \tilde{T}_q and \tilde{P} , respectively. ■

Definition 7 (Symmetric selection policy): For $Q/M \in \mathbb{N}$ and $M\bar{Q}/Q \in \mathbb{N}$, let $\{\mathcal{Q}_m\}_{m=1}^M$ be a partition of \mathcal{Q} , such that $|\mathcal{Q}_m| = Q/M \forall m$. In this selection policy, $\forall m \in \mathcal{M}$, the set of MSs discarded by S-RRH- m is given by $\bar{\mathcal{S}}_m = \bigcup_{i=1}^{\bar{Q}M/Q} \mathcal{Q}_{(i+m) \bmod M}$.

Corollary 8: Consider the assumptions of Theorem 5 and assume in addition that $Q/M \in \mathbb{N}$, $M\bar{Q}/Q \in \mathbb{N}$ and a symmetric selection policy (cf. Definition 7). Then $\Delta \tilde{R} \leq \Delta \tilde{R}_1 + \Delta \tilde{R}_2 +$

ΔR_{AG} , where $\Delta R_{\text{AG}} = \varphi(T, P/M) - \varphi(\tilde{T}, \tilde{P}/M)$, $\tilde{T} = M(1 - \bar{Q}/Q)\tilde{N}_t + 1 - \min(Q, (2 - 1/M)Q - 2\bar{Q})$, and

$$\begin{aligned} \Delta \tilde{R}_1 &= \log \left\{ 1 + \frac{\tilde{P}\tilde{N}_t(Q - \bar{Q} - 1)}{M} \times \left[\frac{1}{\tilde{N}_t - 1} 2^{\frac{-B}{(Q - \bar{Q})(\tilde{N}_t - 1)}} \left(2(1 - \mathcal{U}(2^{\frac{B}{Q - \bar{Q}}}, \tilde{a})) + 2^{\frac{-B}{(Q - \bar{Q})(\tilde{N}_t - 1)}} \right) \right. \right. \\ &\quad \left. \left. + (1 - \mathcal{U}(2^{\frac{B}{Q - \bar{Q}}}, \tilde{a}))^2 - (1 - \mathcal{U}(2^{\frac{B}{Q - \bar{Q}}}, \tilde{a})/2 - \mathcal{U}(2^{\frac{B}{Q - \bar{Q}}}, 2\tilde{a}))^4 \right] \right\} \end{aligned} \quad (34)$$

$$\Delta \tilde{R}_2 = 6\varphi(\tilde{T}, \tilde{P}/M) \left((\mathcal{U}(2^{\frac{B}{Q - \bar{Q}}}, \tilde{a}) + \mathcal{V}_{(1 - \bar{Q}/Q)M}(2^{\frac{B}{Q - \bar{Q}}}, \tilde{a})) \right. \quad (35)$$

$$\begin{aligned} &\quad \left. + \frac{\pi\sqrt{\tilde{P}\tilde{N}_t(1 - \bar{Q}/Q)M}}{\sqrt{2}} U\left(\frac{1}{2}, \frac{1 - \tilde{N}_t(1 - \bar{Q}/Q)M}{2}, \frac{1}{2\tilde{P}}\right) \right. \\ &\quad \left. \times [\mathcal{U}(2^{\frac{B}{Q - \bar{Q}}}, \tilde{a}/2) + \mathcal{V}_{(1 - \bar{Q}/Q)M}(2^{\frac{B}{Q - \bar{Q}}}, \tilde{a}/2)] \right] \end{aligned} \quad (36)$$

Proof: Due to space limitations, we provide here an outline of the proof, whereas the detailed proof is given in Supplementary B. The first step is to show that the sum in (30) runs over constant terms, and therefore can be replaced by a factor $Q - \bar{Q} - 1$ in (34). one must show that $M_q = (1 - \bar{Q}/Q)M, \forall q \in \mathcal{Q}$, as we do in Supplementary B. Finally, we substitute the latter result for \tilde{T}_q in (32) and obtain $\tilde{T}_q = \tilde{T}$, where \tilde{T} is given in this corollary. ■

Remark 4: Under the suppositions of Corollary 8, all MS rates are equal, $\hat{R}_q = \hat{R}$ (cf. Definition 5), and satisfy $\hat{R} \geq R^* - \Delta \tilde{R}_1 - \Delta \tilde{R}_2 - \Delta R_{\text{AG}}$, where R^* is given in (18). Moreover, considering the standard scheme under Assumption 8 and $Q/M \in \mathbb{N}$, it follows that $\hat{R} \geq R^* - \Delta \bar{R}_1 - \Delta \bar{R}_2$.

Next, similar to Corollary 4, we have to following corollary.

Corollary 9: Consider $\Delta \tilde{R}_1$ and $\Delta \tilde{R}_2$, given in Corollary 8. Then the bound $\tilde{\Delta}R \leq \Delta \tilde{R}_1 + \Delta \tilde{R}_2 \Delta + R_{\text{AG}}$ in (29) can be further approximated as

$$\begin{aligned} \Delta \tilde{R}_1 + \Delta \tilde{R}_2 &= 2^{\frac{-B}{2(Q - \bar{Q})(\tilde{N}_t - 1)}} \frac{\pi\sqrt{\tilde{P}\tilde{N}_t(1 - \bar{Q}/Q)M}}{\sqrt{2}} U\left(\frac{1}{2}, \frac{1 - \tilde{N}_t(1 - \bar{Q}/Q)M}{2}, \frac{1}{2\tilde{P}}\right) \\ &\quad \times \left[V_M\left(\frac{1/2}{\tilde{N}_t - 1}\right) + \Gamma\left(\frac{1/2}{\tilde{N}_t - 1} + 1\right) \right] + O(2^{\frac{-2B}{(Q - \bar{Q})(\tilde{N}_t - 1)}}) . \end{aligned} \quad (37)$$

Proof: The proof is identical to the proof of Corollary 4. ■

We conclude this section by a discussion and insights. By examining Corollaries 4 and 9, it follows that the rate loss ΔR in the standard scheme (which here is not a function of q , cf.

Remark 4), approaches zero as B increases, whereas the rate gap in the P&Q scheme, $\Delta\tilde{R}$, is bounded away from zero. Explicitly, it approaches $\Delta R_{\text{AG}} > 0$ (cf. Definition 6), which is independent of B and is due to the array-gain loss induced by the dimension reduction. However the other terms $\Delta\tilde{R}_1 + \Delta\tilde{R}_2$, comprising $\Delta\tilde{R}$, decrease to zero much faster than $\Delta\bar{R}_1 + \Delta\bar{R}_2$ (cf. (21) and (37)); therefore, $\Delta\tilde{R}$ approaches ΔR_{AG} much faster than ΔR approaches zero. Subsequently, $\hat{\tilde{R}}$ approaches $R^* - \Delta R_{\text{AG}}$, much faster than \hat{R} approaches R^* . The final observation is that $\hat{\tilde{R}}$ can be higher than \hat{R} as long as ΔR is more significant than ΔR_{AG} . Numerical results presented in the subsequent section indicate that $\hat{\tilde{R}}$ is indeed higher than \hat{R} for a wide range of quantization bits.

VI. NUMERICAL RESULTS

In this section, we study two setups. The first is a symmetric setup matching the theoretical analysis in sections III and V, where we compare the derived bounds to their corresponding Monte Carlo (MC) simulations (Fig. 2). The second is a practically oriented setup in which the MSs are placed randomly in the plane with a more realistic channel model (cf. Fig. 3).

We begin with the symmetric setup. Here we consider a network satisfying Assumption 8 under the symmetric system policy of Definition 7, with four S-RRHs and eight MSs. We begin with evaluating the standard ZF scheme for two transmitter-SNRs levels; i.e., we set P according to Assumption 6 with $P_{\text{max}} = 15$ dB and $P_{\text{max}} = 35$ dB, and the noise power to one. Fig. 2(a) depicts the standard-scheme performance (ergodic rate), evaluated via MC (300 channel realizations), compared to the rate lower-bound (cf. Remark 4). Also included is the rate under perfect CSI, (cf. (18)). Considering that transmitters could always turn off some of their antennas if it yields a higher rate, for each B we picked $N_t \in \{2, \dots, 8\}$ with the maximum rate. The corresponding bound was also maximized over N_t for each B (cf. Supplementary C for further details). The results show that the bound becomes non-trivial (greater than zero) after a finite number of bits, and gets tighter as B increases. Moreover, the bound exhibits the same behavior as the MC simulation when B increases.

Fig. 2(b) studies the P&Q and the standard schemes for $M = 4$ and $Q = 8$. It depicts the bound of the latter scheme, as in Fig. 2(a) compared to the corresponding bound of the P&Q and collates them to rates obtained via MC (300 realizations) for $P_{\text{max}} = 35$ dB. For the standard scheme, the rate was calculated as in Fig. 2(a), wherein the P&Q scheme was also maximized

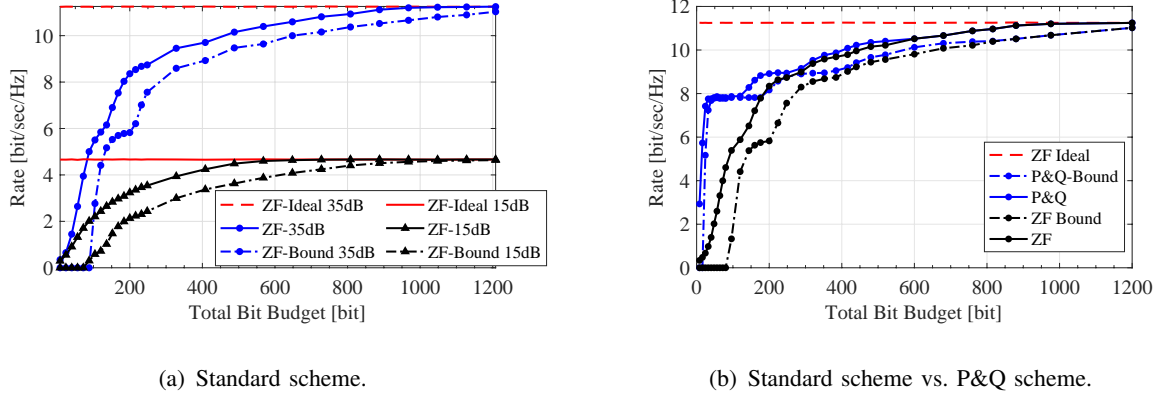


Fig. 2. Lower bounds on the averaged throughput (cf. Remark 4) versus MC simulation, as a function of the overall bit budget B in a symmetric configuration (cf. Assumption 8). The number of MSs is $Q = 8$, and $M = 4$ S-RRHs, each with $N_t = 8$ antennas.

over all feasible values of \bar{Q} (cf. Supplementary C). The result indicates that the P&Q scheme provides a significant performance gain; that is, $\hat{\bar{R}}$ is much greater than \hat{R} for at least 250 bits. Moreover, in the P&Q scheme, the bound is tighter and approaches the MC simulation way faster than the corresponding bound in the standard scheme. Furthermore, it becomes non-trivial only after 20 bits compared to 75 bits in the standard one.

To further investigate the P&Q scheme, we study a practically oriented setup with randomly dispersed MSs while considering propagation loss and shadowing. The setup includes a cluster of $M = 4$ S-RRHs, creating a 100 m edge-length rhombus with an edge angle of 120° (cf. Supplementary C for further details). Each S-RRH is equipped with $N_t = 8$ isotropic transmit antennas. Eight single-antenna MSs ($Q = 8$) were placed uniformly at random in the joint area spanned by four hexagons, each one centered at a different S-RRH. We set a minimum distance of 10 m between each MS and S-RRH. The results were averaged over 20 realizations of MS-placements, where each realization determined a set of attenuation factors $\alpha = \{\alpha_{q,m} : q = 1 \dots 8, m = 1 \dots 4\}$ according $\alpha_{q,m} = -128 - 37.6 \log_{10}(r_{q,m})$ (in dB),¹³ where $r_{q,m}$ is the distance from S-RRH- m to MS- q in Km. The noise level at the receivers was -121 dBm. For each realization of MS-placement, we calculated each MS rate by averaging over 40 channel realizations. In calculating the network throughput, we averaged the rates of all MSs across all

¹³This model was used for urban-area non-line-of-site links by the 3GPP; cf. page 61 3GPP Technical Report 36.814 [33].

placements. To ensure a fair comparison, we considered that the transmitters could always turn off some of their antennas to reduce the effective MISO channel dimensions. Accordingly, in the standard scheme, we maximized the rate over N_t , whereas in the P&Q scheme, we maximized the rate over \bar{Q} , while keeping $N_t = 8$. Finally, we set the overall power transmitted to each MS, as fixed; i.e., $P_q = P_{q'}, \forall q, q' \in \mathcal{Q}$ (cf. (3)). To maintain $\|\mathbf{p}_q\| = 1$, all S-RRH had to backoff its power until none was violating its individual power constraint P_{\max} .¹⁴ A more detailed description of this policy is given in Supplementary C.

Fig. 3(a) presents the throughput as a function of each S-RRH transmit power, P_{\max} (cf. Assumption 2). The results show that the P&Q significantly outperformed the standard scheme. In the latter, the network is already interference limited at 50 dBm, whereas in the former, this does not occur until 110 dBm. Therefore, while the perfect-CSI throughput in the standard scheme is higher than the P&Q counterpart, the latter goes up much faster.

To study the effect of the quantization bits, Fig. 3(b) presents the average throughput as a function of B , under a per-S-RRH power constraint of $P_{\max} = 45$ dBm. The result shows that the P&Q throughput rapidly increases with B ; thus, outperforming the standard scheme for a wide range of B .

VII. CONCLUSIONS

This article makes two contributions. The first is a new upper bound on the rate degradation experienced by a cluster of S-RRHs, that employ joint ZF with incomplete CSI compared to perfect CSI. The second is a new CSI sharing scheme that aims to reduce the CSI overhead on the links between S-RRHs in C-RAN. The key distinguishing characteristic of this scheme is that it applies front-end matrices prior to CSI quantization, to create designated effective channels of low dimensionality; hence can be quantized more accurately with fewer bits. Furthermore, each S-RRH serves fewer MSs, thus reducing the amount of CSI and data streams that must be delivered. We demonstrated, through analytical analysis and simulation that the proposed scheme achieves a significant performance gain.

Possible extensions of this work include other choices of local precoding matrices ($\mathbf{A}_m, m = 1, \dots, M$ cf. (23)). A further direction would be to optimize the power allocation for each MS as

¹⁴Note that while this power allocation strategy is not optimal, it yields good performance in high SNRs.

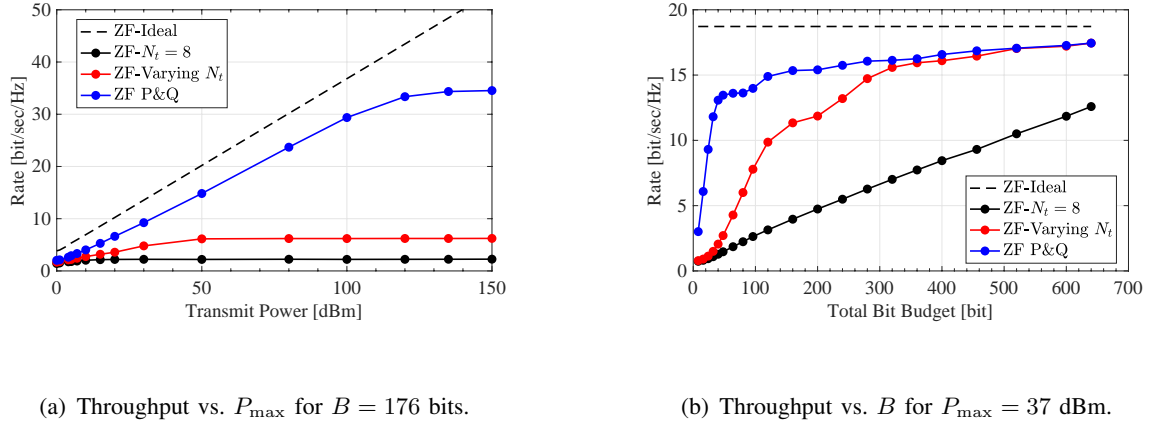
(a) Throughput vs. P_{\max} for $B = 176$ bits.(b) Throughput vs. B for $P_{\max} = 37$ dBm.

Fig. 3. Throughput of the P&Q scheme (blue), standard scheme with varying N_t (red), with fixed $N_t = 8$ (black) and under perfect CSI (dashed). The overall bit budget per S-RRH, B (cf. Assumptions 4 and 5), is allocated equally to each MS; that is, B/Q and $B/(Q - \bar{Q})$ bits per MS in the standard and in the P&Q scheme, respectively, where non-integer values were floored.

well as examining schemes beyond ZF. Finally, it would be important to explore more advanced quantization schemes, where S-RRHs quantize their local CSI jointly.

APPENDIX A

To prove Lemma 2, we begin by rewriting the decomposition in (7) as

$$\bar{\mathbf{h}}_{q,m} = \hat{\bar{\mathbf{h}}}_{q,m} \cos \theta_{q,m} + \mathbf{s}_{q,m} \sin \theta_{q,m}, \quad (38)$$

where $\bar{\mathbf{h}}_{q,m} = \mathbf{h}_{q,m}/\|\mathbf{h}_{q,m}\|$ and $\hat{\bar{\mathbf{h}}}_{q,m} = \hat{\mathbf{h}}_{q,m}/\|\hat{\mathbf{h}}_{q,m}\|$, $\theta_{q,m}$ is the angle between $\bar{\mathbf{h}}_{q,m}$ and $\hat{\bar{\mathbf{h}}}_{q,m}$, and $\mathbf{s}_{q,m} \in \mathbb{C}^{N_t \times 1}$ is a unit-norm random vector that is uniformly distributed over the null space of $\hat{\bar{\mathbf{h}}}_{q,m}$ [9]. Moreover, we define¹⁵

$$\hat{\bar{\mathbf{p}}}_{j,m} = \bar{\mathbf{p}}_{j,m} \cos \phi_{j,m} + \mathbf{g}_{j,m} \sin \phi_{j,m} \quad (39)$$

where $\bar{\mathbf{p}}_{j,m} = \mathbf{p}_{j,m}/\|\mathbf{p}_{j,m}\|$ and $\hat{\bar{\mathbf{p}}}_{j,m} = \hat{\mathbf{p}}_{j,m}/\|\hat{\mathbf{p}}_{j,m}\|$, $\phi_{j,m}$ is the angle between $\bar{\mathbf{p}}_{j,m}$ and $\hat{\bar{\mathbf{p}}}_{j,m}$, and $\mathbf{g}_{j,m} \in \mathbb{C}^{N_t \times 1}$ is a unit-norm random vector that is uniformly distributed over the null space of $\bar{\mathbf{p}}_{j,m}$.

¹⁵Interchanging $\bar{\mathbf{p}}_{j,m}$ and $\hat{\bar{\mathbf{p}}}_{j,m}$ yields an equivalent decomposition of the quantized beamforming vector [34]; furthermore, $\hat{\bar{\mathbf{p}}}_{j,m}$ is uniformly distributed.

Applying Jensen's inequality to A_3 , one obtains

$$A_3 \leq \log \left(1 + P \sum_{j \in \mathcal{Q}_q} \mathbb{E} \{ |\mathbf{h}_q^\dagger \hat{\mathbf{p}}_j|^2 \} \right) \quad (40)$$

and using (38) and (39), the term with the expectation in (40) can be written as

$$\begin{aligned} \mathbb{E} \{ |\mathbf{h}_q^\dagger \hat{\mathbf{p}}_j|^2 \} &= \mathbb{E} \left\{ \left| \sum_{m=1}^M \bar{\mathbf{h}}_{q,m}^\dagger \hat{\mathbf{p}}_{j,m} \|\mathbf{h}_{q,m}\| \|\hat{\mathbf{p}}_{j,m}\| \right|^2 \right\} = \mathbb{E} \left\{ \left| \sum_{m=1}^M \left(\hat{\mathbf{h}}_{q,m}^\dagger \mathbf{p}_{j,m} \Lambda_{1,1m} \right. \right. \right. \\ &\quad \left. \left. \left. + \hat{\mathbf{h}}_{q,m}^\dagger \mathbf{g}_{j,m} \|\hat{\mathbf{p}}_{j,m}\| \Lambda_{1,2m} + \mathbf{s}_{q,m}^\dagger \mathbf{p}_{j,m} \|\mathbf{h}_{q,m}\| \Lambda_{2,1m} + \mathbf{s}_{q,m}^\dagger \mathbf{g}_{j,m} \|\mathbf{h}_{q,m}\| \|\hat{\mathbf{p}}_{j,m}\| \Lambda_{2,2m} \right) \right|^2 \right\} \end{aligned} \quad (41)$$

where $\Lambda_{k,l_m} = C_k(\theta_{q,m}) C_l(\phi_{j,m})$, $k, l \in \{1, 2\}$ and $C_1(\theta) = \cos \theta$, $C_2(\theta) = \sin \theta$. Extending (41), one obtains

$$\mathbb{E} \{ |\mathbf{h}_q^\dagger \hat{\mathbf{p}}_j|^2 \} = D + E + F + G + H \quad (42)$$

where $D = \mathbb{E} \{ \left| \sum_{m=1}^M \hat{\mathbf{h}}_{q,m}^\dagger \mathbf{p}_{j,m} \Lambda_{1,1m} \right|^2 \}$, $E = \mathbb{E} \{ \left| \sum_{m=1}^M \hat{\mathbf{h}}_{q,m}^\dagger \mathbf{g}_{j,m} \|\hat{\mathbf{p}}_{j,m}\| \Lambda_{1,2m} \right|^2 \}$, $F = \mathbb{E} \{ \left| \sum_{m=1}^M \mathbf{s}_{q,m}^\dagger \mathbf{p}_{j,m} \|\mathbf{h}_{q,m}\| \Lambda_{2,1m} \right|^2 \}$, $G = \mathbb{E} \{ \left| \sum_{m=1}^M \mathbf{s}_{q,m}^\dagger \mathbf{g}_{j,m} \|\mathbf{h}_{q,m}\| \|\hat{\mathbf{p}}_{j,m}\| \Lambda_{2,2m} \right|^2 \}$ and $H = \sum_{i=1}^{12} \Xi_i$ in which $\{\Xi_i\}_{i=1}^{12}$ includes all non-quadratic terms resulting from the extension of the right hand side (r.h.s.) of (41); i.e., terms that cannot be written as $|\cdot|^2$. For example, Ξ_1 is given by

$$\Xi_1 = \mathbb{E} \left\{ \sum_{m=1}^M \sum_{n=1}^M \hat{\mathbf{h}}_{q,m}^\dagger \mathbf{p}_{j,m} \mathbf{g}_{j,n}^\dagger \hat{\mathbf{h}}_{q,n} \|\hat{\mathbf{p}}_{j,n}\| \Lambda_{1,1m} \Lambda_{1,2n} \right\} \quad (43)$$

Proposition 10: The term D , in (42), satisfies

$$D \leq \frac{N_t}{M} \left((1 - \mathcal{U}(2^{B/Q}, a))^2 - (1 - \mathcal{U}(2^{B/Q}, a)/2 - \mathcal{U}(2^{B/Q}, 2a))^4 \right) \quad (44)$$

where $a = \frac{1}{N_t-1}$ and $\mathcal{U}(\cdot)$ is defined in (16).

Proof: Because $\{\Lambda_{1,1m}\}_{m \in \mathcal{M}}$ are identically distributed, it can be written as $\Lambda_{1,1m} = \sigma + \bar{\Lambda}_{1,1m}$, $\forall m \in \mathcal{M}$, where $\mathbb{E} \{ \bar{\Lambda}_{1,1m} \} = 0$ and $\sigma = \mathbb{E} \{ \Lambda_{1,1m} \}$. Substituting $\Lambda_{1,1m}$ into D (cf. (42)) while recalling that $\{\theta_{q,i}, \phi_{j,i}\}_{i \in \mathcal{M}, q, j \in \mathcal{Q}}$, are independent of $\{\hat{\mathbf{h}}_{q,i}, \mathbf{p}_{j,i}\}_{i \in \mathcal{M}, q, j \in \mathcal{Q}}$, it can be shown that

$$D = \sigma^2 \mathbb{E} \left\{ \left| \hat{\mathbf{h}}_q^\dagger \mathbf{p}_j \right|^2 \right\} + \mathbb{E} \left\{ \left| \sum_{m=1}^M \hat{\mathbf{h}}_{q,m}^\dagger \mathbf{p}_{j,m} \bar{\Lambda}_{1,1m} \right|^2 \right\} \quad (45)$$

$$+ \sigma \sum_{m=1}^M \sum_{n=1}^M \mathbb{E} \left\{ \hat{\mathbf{h}}_{q,m}^\dagger \mathbf{p}_{j,m} \mathbf{p}_{j,n}^\dagger \hat{\mathbf{h}}_{q,n} \right\} \mathbb{E} \{ \bar{\Lambda}_{1,1n} \} + \sigma \sum_{m=1}^M \sum_{n=1}^M \mathbb{E} \left\{ \hat{\mathbf{h}}_{q,m}^\dagger \mathbf{p}_{j,m} \mathbf{p}_{j,n}^\dagger \hat{\mathbf{h}}_{q,n} \right\} \mathbb{E} \{ \bar{\Lambda}_{1,1m} \}$$

$$= \mathbb{E} \left\{ \left| \sum_{m=1}^M \hat{\mathbf{h}}_{q,m}^\dagger \mathbf{p}_{j,m} \bar{\Lambda}_{1,1m} \right|^2 \right\} \quad (46)$$

To obtain the latter, we also used $\hat{\mathbf{h}}_q^\dagger \mathbf{p}_j = 0$, $\forall j \neq q \in \mathcal{Q}$ and $\mathbb{E}\{\bar{\Lambda}_{1,1_m}\} = 0$. Now, (46) can be written as

$$D = \mathbb{E} \left\{ \sum_{m=1}^M |\hat{\mathbf{h}}_{q,m}^\dagger \mathbf{p}_{j,m}|^2 \bar{\Lambda}_{1,1_m}^2 \right\} + \mathbb{E} \left\{ \sum_{m=1}^M \sum_{n \neq m}^M \hat{\mathbf{h}}_{q,m}^\dagger \mathbf{p}_{j,m} \mathbf{p}_{j,n}^\dagger \hat{\mathbf{h}}_{q,n} \bar{\Lambda}_{1,1_m} \bar{\Lambda}_{1,1_n} \right\} \quad (47)$$

$$= \sum_{m=1}^M \underbrace{\mathbb{E}\{\|\mathbf{p}_{j,m}\|^2 \|\hat{\mathbf{h}}_{q,m}\|^2 |\hat{\mathbf{h}}_{q,m}^\dagger \bar{\mathbf{p}}_{j,m}|^2\}}_{I_{q,m}} \underbrace{\mathbb{E}\{\bar{\Lambda}_{1,1_m}^2\}}_J \quad (48)$$

where we again used the independence between $\{\theta_{q,i}, \phi_{j,i}\}_{i \in \mathcal{M}, q,j \in \mathcal{Q}}$ and $\{\hat{\mathbf{h}}_{q,i}, \mathbf{p}_{j,i}\}_{i \in \mathcal{M}, q,j \in \mathcal{Q}}$ as well as the independence between $\bar{\Lambda}_{1,1_m}$ and $\bar{\Lambda}_{1,1_n} \forall m \neq n \in \mathcal{M}$.

Next, using $I_{q,m} = \sqrt{I_{q,m}^2}$ and applying the Cauchy-Schwarz inequality, one obtains

$$I_{q,m} \leq \sqrt{\mathbb{E}^2\{\|\mathbf{p}_{j,m}\|^2\} \mathbb{E}^2\{\|\hat{\mathbf{h}}_{q,m}\|^2\} \mathbb{E}^2\{|\hat{\mathbf{h}}_{q,m}^\dagger \bar{\mathbf{p}}_{j,m}|^2\}} \stackrel{(a)}{=} \frac{\alpha_{q,m} N_t}{M} \mathbb{E}\{|\hat{\mathbf{h}}_{q,m}^\dagger \bar{\mathbf{p}}_{j,m}|^2\} \stackrel{(b)}{\leq} \frac{\alpha_{q,m} N_t}{M} \quad (49)$$

where in (a) we used Assumption 1, $\mathbb{E}\{\|\hat{\mathbf{h}}_{q,m}\|^2\}/\alpha_{q,m} = N_t$ [9], and $\mathbb{E}\{\|\mathbf{p}_{j,m}\|^2\} = \frac{1}{M}$. The latter follows because $\|\mathbf{p}_j\|^2 = 1$ and $\{\|\mathbf{p}_{j,m}\|\}_{m \in \mathcal{M}}$ are identically distributed. In (b) we used $\mathbb{E}\{|\hat{\mathbf{h}}_{q,m}^\dagger \bar{\mathbf{p}}_{j,m}|^2\} \leq 1$. Proceeding to J (cf. (48)), note that

$$\begin{aligned} J &= \mathbb{E}\{(\Lambda_{1,1_m} - \mathbb{E}\{\Lambda_{1,1_m}\})^2\} = \mathbb{E}\{\cos^2 \theta_{q,m} \cos^2 \phi_{j,m}\} - (\mathbb{E}\{\cos \theta_{q,m} \cos \phi_{j,m}\})^2 \\ &= \mathbb{E}^2\{\cos^2 \theta_{q,m}\} - \mathbb{E}^4\{\cos \theta_{q,m}\}, \end{aligned} \quad (50)$$

where the latter follows since $\theta_{q,m}$ and $\phi_{j,m}$, $\forall m \in \mathcal{M}$, $q, j \in \mathcal{Q}$, are independent identically distributed. Because $\mathbf{h}_{q,m}$ is quantized with B/Q bits, it follows that [9]

$$\mathbb{E}\{\cos^2 \theta_{q,m}\} = 1 - \mathcal{U}(2^{B/Q}, a) \quad (51)$$

where \mathcal{U} is defined in (16). Before continuing, note that

$$\mathbb{E}\{\cos \theta_{q,m}\} \geq 1 - \mathcal{U}(2^{B/Q}, a)/2 - \mathcal{U}(2^{B/Q}, 2a) \quad (52)$$

where we used $\cos \theta_{q,m} = \sqrt{1 - \sin^2(\theta_{q,m})}$ and the inequality $\sqrt{1 - x} \geq 1 - x/2 - x^2$, $\forall x \in [0, 1]$. Thus,

$$J \leq (1 - \mathcal{U}(2^{B/Q}, a))^2 - (1 - \mathcal{U}(2^{B/Q}, a)/2 - \mathcal{U}(2^{B/Q}, 2a))^4 \quad (53)$$

which together with $\sum_{m=1}^M \alpha_{q,m} = 1$ (cf. the suppositions of Theorem 1) establishes the desired result. \blacksquare

Proposition 11: The terms E and F , given in (42), satisfy

$$E, F \leq \frac{N_t}{M(N_t - 1)} (1 - \mathcal{U}(2^{B/Q}, a)) 2^{\frac{-B}{Q(N_t - 1)}} \quad (54)$$

Proof: Rewriting E (cf. (42)) one obtains

$$E = \mathbb{E} \left\{ \sum_{m=1}^M \left| \hat{\mathbf{h}}_{q,m}^\dagger \mathbf{g}_{j,m} \|\hat{\mathbf{p}}_{j,m}\|^2 \Lambda_{1,2m}^2 \right| \right\} \quad (55)$$

$$+ \mathbb{E} \left\{ \sum_{m=1}^M \sum_{n \neq m}^M \hat{\mathbf{h}}_{q,m}^\dagger \mathbf{g}_{j,m} \mathbf{g}_{j,n}^\dagger \hat{\mathbf{h}}_{q,n} \|\hat{\mathbf{p}}_{j,m}\| \|\hat{\mathbf{p}}_{j,n}\| \Lambda_{1,2m} \Lambda_{1,2n} \right\} \quad (56)$$

Now, denote

$$w = \hat{\mathbf{h}}_{q,m}, \mathbf{g}_{j,n}, \hat{\mathbf{h}}_{q,n}, \|\mathbf{h}_{q,m}\|, \|\mathbf{h}_{q,n}\|, \|\hat{\mathbf{p}}_{j,m}\|, \|\hat{\mathbf{p}}_{j,n}\| \quad (57)$$

and using the same independence argument as in (45), the double sum in (56) can be written as

$$\sum_{m=1}^M \sum_{n \neq m}^M \mathbb{E} \left\{ \mathbb{E} \left\{ \hat{\mathbf{h}}_{q,m}^\dagger \mathbf{g}_{j,m} \mathbf{g}_{j,n}^\dagger \hat{\mathbf{h}}_{q,n} \|\hat{\mathbf{p}}_{j,m}\| \|\hat{\mathbf{p}}_{j,n}\| \middle| \bar{\mathbf{p}}_{j,m}, w \right\} \right\} \mathbb{E} \left\{ \Lambda_{1,2m} \Lambda_{1,2n} \right\} \quad (58)$$

Given w , all the arguments inside the internal expectation are constants, except $\mathbf{g}_{j,m}$. Furthermore, recalling that given $\bar{\mathbf{p}}_{j,m}$, $\mathbf{g}_{j,m}$ is uniformly distributed on the unit sphere of the null space of $\bar{\mathbf{p}}_{j,m}$, it follows that $\mathbb{E} \{ \mathbf{g}_{j,m} | \bar{\mathbf{p}}_{j,m}, w \} = \mathbf{0}_{N_t}$. Thus, the double sum in (56) is equal to zero. Applying the Cauchy-Schwarz inequality to (55) and using again the independence argument as in (45), one obtains

$$E \leq \sum_{m=1}^M \mathbb{E} \left\{ \left| \hat{\mathbf{h}}_{q,m}^\dagger \mathbf{g}_{j,m} \right|^2 \right\} \mathbb{E} \left\{ \|\mathbf{h}_{q,m}\|^2 \right\} \mathbb{E} \left\{ \|\hat{\mathbf{p}}_{j,m}\|^2 \right\} \mathbb{E} \left\{ \Lambda_{1,2m}^2 \right\}. \quad (59)$$

Next, from (59),

$$E \leq \frac{N_t}{M} \mathbb{E} \left\{ \left| \hat{\mathbf{h}}_{q,m}^\dagger \mathbf{g}_{j,m} \right|^2 \right\} \mathbb{E} \left\{ \cos^2 \theta_{q,m} \right\} \mathbb{E} \left\{ \sin^2 \phi_{j,m} \right\} \quad (60)$$

where we used similar arguments as in (50) with respect to the angles, and in addition, $\mathbb{E} \{ \|\bar{\mathbf{h}}_{q,m}\|^2 \} / \alpha_{q,m} = N_t$ [9], $\sum_{m=1}^M \alpha_{q,m} = 1$, and $\mathbb{E} \{ \|\hat{\mathbf{p}}_{j,m}\|^2 \} = \frac{1}{M}$.

To further simplify (60), we treat each of the expressions in the r.h.s. separately. We begin with

$$\mathbb{E} \{ \cos^2 \theta_{q,m} \} \mathbb{E} \{ \sin^2 \phi_{j,m} \} \leq (1 - \mathcal{U}(2^{B/Q}, a)) 2^{\frac{-B}{Q(N_t - 1)}} \quad (61)$$

where we used (51) as well as the upper bound [9]

$$\mathbb{E} \{ \sin^2 \phi_{j,m} \} \leq 2^{\frac{-B}{Q(N_t - 1)}}. \quad (62)$$

Next, consider $\hat{\mathbf{h}}_{q,m} = \mathbf{P}_{\mathbf{g}_{j,m}} \hat{\mathbf{h}}_{q,m} + \mathbf{P}_{\mathbf{g}_{j,m}}^\perp \hat{\mathbf{h}}_{q,m}$, where $\mathbf{P}_{\mathbf{g}_{j,m}}$, $\mathbf{P}_{\mathbf{g}_{j,m}}^\perp$ are the projection matrices into space spanned by $\mathbf{g}_{j,m}$ and into its orthogonal complement, respectively. It follows that

$$\begin{aligned} \mathbb{E}\left\{|\hat{\mathbf{h}}_{q,m}^\dagger \mathbf{g}_{j,m}|^2\right\} &= \mathbb{E}\left\{|\left((\mathbf{P}_{\mathbf{g}_{j,m}} \hat{\mathbf{h}}_{q,m})^\dagger + (\mathbf{P}_{\mathbf{g}_{j,m}}^\perp \hat{\mathbf{h}}_{q,m})^\dagger\right) \mathbf{g}_{j,m}|^2\right\} \\ &\stackrel{(a)}{=} \mathbb{E}\left\{|\left(\mathbf{P}_{\mathbf{g}_{j,m}} \hat{\mathbf{h}}_{q,m}\right)^\dagger \mathbf{g}_{j,m}|^2\right\} \stackrel{(b)}{\leq} \mathbb{E}\left\{\left|\frac{(\mathbf{P}_{\mathbf{g}_{j,m}} \hat{\mathbf{h}}_{q,m})^\dagger}{\|\mathbf{P}_{\mathbf{g}_{j,m}} \hat{\mathbf{h}}_{q,m}\|} \mathbf{g}_{j,m}\right|^2\right\} \stackrel{(c)}{=} \frac{1}{N_t - 1} \end{aligned} \quad (63)$$

where (a) follows because $\mathbf{P}_{\mathbf{g}_{j,m}}^\perp \mathbf{g}_{j,m} = \mathbf{0}_{N_t}$ and (b) follows from $\|\mathbf{P}_{\mathbf{g}_{j,m}} \hat{\mathbf{h}}_{q,m}\| \leq 1$ (recall that $\|\hat{\mathbf{h}}_{q,m}\| = 1$). (c) follows because $\mathbf{g}_{j,m}$ is independent of $\mathbf{P}_{\mathbf{g}_{j,m}} \hat{\mathbf{h}}_{q,m}$, and is uniformly distributed on the unit sphere of the $(N_t - 1)$ -dimensional null space of $\bar{\mathbf{p}}_{j,m}$. Thus, the expectation on the left hand side of (c) is taken according to the $\beta(1, N_t - 2)$ distribution [9].

Substituting (61) and (63), into (60), establishes (54) with respect to E . The proof for F is identical and is omitted here due to space limitations. \blacksquare

Proposition 12: The term G in (42) satisfies $G \leq \frac{N_t}{M(N_t-1)} 2^{-\frac{2B}{Q(N_t-1)}}$.

Proof: Similar to the derivation of (59), it can be shown that

$$G \leq \sum_{m=1}^M \mathbb{E}\left\{|\mathbf{s}_{q,m}^\dagger \mathbf{g}_{j,m}|^2\right\} \mathbb{E}\left\{\|\mathbf{h}_{q,m}\|^2\right\} \mathbb{E}\left\{\|\hat{\mathbf{p}}_{j,m}\|^2\right\} \mathbb{E}\left\{\Lambda_{2,2m}^2\right\}. \quad (64)$$

Next, $\mathbb{E}\{|\mathbf{s}_{q,m}^\dagger \mathbf{g}_{j,m}|^2\}$ can be bounded using similar arguments as in (63), and by further employing (62), one obtains the desired result. \blacksquare

Proposition 13: Consider $H = \{\Xi_i\}_{i=1}^{12}$ (cf. (42)), then $\Xi_i = 0$, $\forall i \in \{1 \dots 12\}$.

Proof: The proposition will be proven only for Ξ_1 , where for the rest Ξ_i , $i > 1$ the proof is identical. Similar to (58), and with $w = \hat{\mathbf{h}}_{q,m}, \bar{\mathbf{p}}_{j,m}, \hat{\mathbf{h}}_{q,n}, \|\mathbf{h}_{q,m}\|, \|\mathbf{h}_{q,n}\|, \|\hat{\mathbf{p}}_{j,m}\|, \|\hat{\mathbf{p}}_{j,n}\|$ it can be shown that $\mathbb{E}\{\mathbf{g}_{j,n}^\dagger \bar{\mathbf{p}}_{j,n}, w\} = \mathbf{0}_{N_t}$. Thus, $\Xi_1 = 0$, which establishes the desired result. \blacksquare

To complete the proof, we apply Propositions 10, 11, 12, 13 to (42), and in turn, substitute the result in (40), which establishes the desired result.

APPENDIX B

The proof of Lemma 6 is similar to the proof of Lemma 2 (cf. Appendix A). It is obtained by substituting $\tilde{\mathbf{h}}_q, \hat{\mathbf{h}}_q, \tilde{\mathbf{p}}_j, \hat{\mathbf{p}}_j, \tilde{\mathbf{s}}_{q,m}, \tilde{\mathbf{g}}_{j,m}, \tilde{P}, B/(Q - \bar{Q})$ for $\mathbf{h}_q, \hat{\mathbf{h}}_q, \mathbf{p}_j, \hat{\mathbf{p}}_j, \mathbf{s}_{q,m}, \mathbf{g}_{j,m}, P, B/Q$, respectively. Moreover, because $\mathbb{E}\{\|\hat{\mathbf{h}}_{q,m}\|^2\}/\alpha_{q,m} = \tilde{N}_t$ [9], N_t, a are replaced by \tilde{N}_t, \tilde{a} , respectively, and $\alpha_{q,m}$ by $1/M$, due to Assumption 8. The desired result then follows similarly with few caveats as follows.

The sums in (41), (42), (45)-(48), (55), (59), (64) now run over $\mathcal{M}_{q,j}$, (cf. Definition 4), rather than \mathcal{M} ; that is, $\sum_{m=1}^M(\cdot)$ is replaced with $\sum_{m \in \mathcal{M}_{q,j}}(\cdot)$. Similarly, the double sums in (43), (45), (47), (56), (58) now run over $m, n \in \mathcal{M}_{q,j}$. Furthermore, because $E\{\|\tilde{\mathbf{p}}_{j,m}\|^2\} = \frac{1}{M_j}$, the term M in (49), (60) is now changed to M_j . These modifications, as well as Assumption 8 imply that $\sum_{m \in \mathcal{M}_{q,j}} \alpha_{q,m} = M_{q,j}/M$, which thus affect Propositions 10 to 12 in which $1/M$ is replaced with $M_{q,j}/M_j M$.

APPENDIX C

To prove Lemma 3, we begin by bounding A_2 (cf. (19)). Let $\theta_q = \angle(\bar{\mathbf{h}}_q, \hat{\mathbf{h}}_q)$ where $\bar{\mathbf{h}}_q = \mathbf{h}_q/\|\mathbf{h}_q\|$ (cf. (2)), $\hat{\mathbf{h}}_q = \hat{\mathbf{h}}_q/\|\hat{\mathbf{h}}_q\|$ (cf. (5)) and $\xi_q = \angle(\hat{\mathbf{h}}_q, \hat{\mathbf{p}}_q)$. Since the argument of the logarithm in A_2 is always positive; i.e., $|\bar{\mathbf{h}}_q^\dagger \hat{\mathbf{p}}_q| > 0$, we assume without loss of generality that $\angle(\bar{\mathbf{h}}_q, \hat{\mathbf{p}}_q) \in [0, \pi/2]$. Employing the triangle inequality for angles, one obtains,

$$\angle(\bar{\mathbf{h}}_q, \hat{\mathbf{p}}_q) \leq \theta_q + \xi_q \quad (65)$$

Applying $\cos^2(\cdot)$ on both sides, is possible if $0 \leq \xi_q + \theta_q \leq \frac{\pi}{2}$, which guarantees the monotonicity of the cosine. Denote the common probability space, in which all random variables we are dealing with are defined, by $(\Omega, \mathcal{F}, \mathbb{P})$, and let

$$\mathcal{A}_q = \{\omega \in \Omega : 0 \leq \xi_q(\omega) + \theta_q(\omega) \leq \frac{\pi}{2}\}. \quad (66)$$

Furthermore for X , a random variable defined on $(\Omega, \mathcal{F}, \mathbb{P})$ and for $\mathcal{A} \in \mathcal{F}$, we denote the random variable $\chi_{\mathcal{A}}(\omega)X(\omega)$ by $\chi_{\mathcal{A}}X$. Combining (66) and (65), it follows that

$$|\bar{\mathbf{h}}_q^\dagger \hat{\mathbf{p}}_q|^2 = \cos^2(\angle(\bar{\mathbf{h}}_q, \hat{\mathbf{p}}_q)) \geq \chi_{\mathcal{A}_q} \cos^2(\angle(\bar{\mathbf{h}}_q, \hat{\mathbf{p}}_q)) \geq \chi_{\mathcal{A}_q} \cos^2(\xi_q + \theta_q) \quad (67)$$

and from the definition of A_2 (cf. (19)) and the monotonicity of $\log(\cdot)$, it follows that

$$A_2 \geq E\{\chi_{\mathcal{A}_q} \log(1 + P\|\mathbf{h}_q\|^2 \cos^2(\xi_q + \theta_q))\}. \quad (68)$$

Proposition 14:

$$\log(1 + P\|\mathbf{h}_q\|^2 \cos^2(\xi_q + \theta_q)) \geq \log(1 + P\|\mathbf{h}_q\|^2 \cos^2(\xi_q)) - \sin(\theta_q)K(P\|\mathbf{h}_q\|^2) \quad (69)$$

where $K(x) \triangleq \frac{\pi x}{2\sqrt{x+1}}$.

Proof: Let $\check{P} = P\|\mathbf{h}_q\|^2$ and $g(\theta, \xi) \triangleq \log(1 + \check{P} \cos^2(\theta + \xi))$ for $\theta, \xi \in [0, \pi/2]$, where for brevity we omit the subscript q in this proof. To bound $g(\theta, \xi)$, we solve $g^{(2,0)}(\theta, \xi) = 0$, from which the inflection point is given by $\theta_I = \cos^{-1}((1/\check{P} + 2)^{1/2}) - \xi$ and $g^{(1,0)}(\theta_I, \xi) = -\check{P}(\check{P} + 1)^{-1/2}$. Furthermore, it can be shown that $g(\theta, \xi)$ is convex for $\theta > \theta_I$ and concave otherwise. We first derive a bound for the case where $\theta_I \leq 0$, in which $g(\theta, \xi)$ is convex for $\theta \in [0, \pi/2]$ and therefore, $g(\theta, \xi) \geq \theta g^{(1,0)}(0, \xi) + g(0, \xi)$. Moreover, it can be shown that $g^{(1,0)}(\theta, \xi) < 0, \forall \theta + \xi < \frac{\pi}{2}$. Then, using $\frac{\pi}{2} \sin(\theta) > \theta$ we replace θ with $\frac{\pi}{2} \sin(\theta)$ and obtain $g(\theta, \xi) \geq \frac{\pi}{2} \sin(\theta) g^{(1,0)}(0, \xi) + g(0, \xi)$. Noting that $g^{(1,0)}(0, \xi) = -\frac{2\check{P} \sin(\xi) \cos(\xi)}{\check{P} \cos^2(\xi) + 1} \geq -\check{P}(\check{P} + 1)^{-1/2}$ and substituting $g(0, \xi)$ into the latter inequality, we obtain (69), which establishes the result for $\theta_I \leq 0$. In the case where $\theta_I > 0$, we use the Lipschitz continuity; i.e., a function $f(x)$ is Lipschitz continuous if $\exists C > 0$ such that $|f(x_1) - f(x_2)| \leq C|x_1 - x_2| \forall x_1, x_2$. If $f(x)$ is differentiable, then $C = \sup_x |df(x)/dx|$. Since $g(\theta, \xi)$ is Lipschitz continuous, by replacing C with the inflection point, one obtains $g(\theta, \xi) \geq g(0, \xi) + \frac{\pi}{2} \sin(\theta) g^{(1,0)}(\theta_I, \xi) = \log(1 + \check{P} \cos^2(\xi)) - \sin(\theta) K(\check{P})$. Finally, because the bounds for $\theta_I \leq 0$ and $\theta_I > 0$ are identical the desired result follows. \blacksquare

Substituting (69) into (68) it follows that

$$A_2 \geq E_2 - \mathbb{E}\{\chi_{\mathcal{A}_q} \sin(\theta_q) K(P\|\mathbf{h}_q\|^2)\} \quad (70)$$

where $E_2 = \mathbb{E}\{\chi_{\mathcal{A}_q} \log(1 + P\|\mathbf{h}_q\|^2 \cos^2 \xi_q)\}$.

Let $\check{\mathbf{h}}_{q,m} = \frac{\mathbf{h}_{q,m}}{\sqrt{\alpha_{q,m}}}$, $\check{\mathbf{h}}_q = [\check{\mathbf{h}}_{q,1} \dots \check{\mathbf{h}}_{q,M}]$. Then, recalling $\alpha_q = 1$ (cf. the suppositions of Theorem 1), it follows $\|\check{\mathbf{h}}_q\|^2 \geq \|\mathbf{h}_q\|^2$. Furthermore, it can be shown that $K(x)$ is monotonically increasing for $x \geq 0$ and therefore $K(P\|\mathbf{h}_q\|^2) \leq K(P\|\check{\mathbf{h}}_q\|^2)$. Noting that $\|\check{\mathbf{h}}_q\|^2$ is chi-square distributed, it can be shown that

$$A_2 \geq E_2 - \mathbb{E}\{\chi_{\mathcal{A}_q}\} \mathbb{E}\{\sqrt{Z_q}\} \frac{\pi \sqrt{P} N_t M}{2\sqrt{2}} U\left(\frac{1}{2}, \frac{1 - N_t M}{2}, \frac{1}{2P}\right) \quad (71)$$

where we substituted $\sin(\theta_q) = \sqrt{Z_q}$, and used the Cauchy-Schwarz inequality for $\mathbb{E}\{\chi_{\mathcal{A}_q}\}$ and $\mathbb{E}\{\sqrt{Z_q}\}$. To bound the term E_2 (cf. (70)) we invoke, once again, the triangular inequity for angles, $\xi_q \leq \phi_q + \angle\langle \hat{\mathbf{h}}_q, \mathbf{p}_q \rangle$, where $\phi_q = \angle\langle \mathbf{p}_q, \hat{\mathbf{p}}_q \rangle$, and obtain

$$E_2 \geq \mathbb{E}\left\{\chi_{\mathcal{C}_q} \log\left(1 + P\|\mathbf{h}_q\|^2 \cos^2(\angle\langle \hat{\mathbf{h}}_q, \mathbf{p}_q \rangle + \phi_q)\right)\right\} \quad (72)$$

where $\mathcal{C}_q = \mathcal{A}_q \cap \mathcal{B}_q$ and $\mathcal{B}_q = \{\omega \in \Omega : 0 \leq \angle(\hat{\mathbf{h}}_q, \mathbf{p}_q)(\omega) + \phi_q(\omega) \leq \frac{\pi}{2}\}$. Using similar arguments as in (69)-(71) it can be shown that

$$\begin{aligned} E_2 \geq & \mathbb{E}\{\chi_{\mathcal{C}_q} \log(1 + P\|\mathbf{h}_q\|^2 \cos^2(\angle(\hat{\mathbf{h}}_q, \mathbf{p}_q)))\} \\ & - \mathbb{E}\{\chi_{\mathcal{C}_q}\} \mathbb{E}\{\sin(\phi_q)\} \frac{\pi\sqrt{P}N_tM}{2\sqrt{2}} U\left(\frac{1}{2}, \frac{1-N_tM}{2}, \frac{1}{2P}\right). \end{aligned} \quad (73)$$

Before continuing, the following proposition is necessary.

Proposition 15: Let $Z_q = \sin^2(\theta_q)$. Then, $Z_q^{\min} \leq Z_q \leq Z_q^{\max}$, where $Z_q^{\min} = \min\{Z_{q,l}, l \in \mathcal{M}\}$ and $Z_q^{\max} = \max\{Z_{q,l}, l \in \mathcal{M}\}$. Moreover,

$$\mathcal{U}(2^{B/Q}, a/2) - \mathcal{V}_M(2^{B/Q}, a/2) \leq \mathbb{E}\{\sqrt{Z_q}\} \leq \mathcal{U}(2^{B/Q}, a/2) + \mathcal{V}_M(2^{B/Q}, a/2) \quad (74)$$

where $\mathcal{U}(\cdot)$ and $\mathcal{V}_M(\cdot)$ are defined in (16) and (17), respectively.

Proof: Consider $Z_q = 1 - \frac{|\hat{\mathbf{h}}_q^\dagger \mathbf{h}_q|^2}{\|\mathbf{h}_q\|^2 \|\hat{\mathbf{h}}_q\|^2} = \sum_{u=1}^M \sum_{l=1}^M \frac{\|\mathbf{h}_{q,l}\|^2 \|\hat{\mathbf{h}}_{q,u}\|^2}{\|\mathbf{h}_q\|^2 \|\hat{\mathbf{h}}_q\|^2} \left(1 - \sqrt{1 - Z_{q,l}} \sqrt{1 - Z_{q,u}}\right)$

where we used (2), (5) and (7). Thus,

$$Z_q \leq \frac{1}{\|\mathbf{h}_q\|^2 \|\hat{\mathbf{h}}_q\|^2} \sum_{u=1}^M \sum_{l=1}^M \|\mathbf{h}_{q,l}\|^2 \|\hat{\mathbf{h}}_{q,u}\|^2 \left(1 - \left(\min\{\sqrt{1 - Z_{q,l}}, l \in \mathcal{M}\}\right)^2\right) = Z_q^{\max}$$

Similarly, it can be shown that $Z_q \geq Z_q^{\min}$, which establishes the first statement of the theorem.

The second statement (cf. (74)) follows from the identities, $\mathbb{E}\{Z_q^{\max}\} \leq \mathbb{E}\{Z_{q,l}\} + \frac{(M-1)\sqrt{\text{var}\{Z_{q,l}\}}}{\sqrt{2M-1}}$, $\mathbb{E}\{Z_q^{\min}\} \geq \mathbb{E}\{Z_{q,l}\} - \frac{(M-1)\sqrt{\text{var}\{Z_{q,l}\}}}{\sqrt{2M-1}}$ (cf. [35], Sec. 4.2). \blacksquare

Note that $\sin(\theta_q)$ and $\sin(\phi_q)$ are identically distributed; therefore, the expression in Proposition 15 also applies to $\sin(\phi_q)$.

Returning to the main proof; by invoking Proposition 15 and combining the latter with (71) and (73), one obtains

$$A_2 \geq \mathbb{E}\{\chi_{\mathcal{C}_q} \log(1 + P|\hat{\mathbf{h}}_q^\dagger \mathbf{p}_q|^2)\} - (\mathbb{E}\{\chi_{\mathcal{A}_q}\} + \mathbb{E}\{\chi_{\mathcal{C}_q}\}) \frac{\pi\sqrt{P}N_tM}{2\sqrt{2}} \quad (75)$$

$$\times U\left(\frac{1}{2}, \frac{1-N_tM}{2}, \frac{1}{2P}\right) [\mathcal{U}(2^{B/Q}, a/2) + \mathcal{V}_M(2^{B/Q}, a/2)] \quad (76)$$

It therefore follows that

$$A_1 - A_2 \leq \mathbb{E}\{(1 - \chi_{\mathcal{C}_q})\} \mathbb{E}\{\log(1 + P|\hat{\mathbf{h}}_q^\dagger \mathbf{p}_q|^2)\} \quad (77)$$

$$+ \frac{\pi\sqrt{P}N_tM}{\sqrt{2}} U\left(\frac{1}{2}, \frac{1-N_tM}{2}, \frac{1}{2P}\right) [\mathcal{U}(2^{B/Q}, a/2) + \mathcal{V}_M(2^{B/Q}, a/2)] \quad (78)$$

where in (77) we used the fact that $|\hat{\mathbf{h}}_q^\dagger \mathbf{p}_q|^2$ and $|\hat{\mathbf{h}}_q^\dagger \mathbf{p}_q^*|^2$ are identically distributed and the Cauchy-Schwarz inequality and in (78) we used $0 \leq \mathbb{E}\{\chi_{\mathcal{A}_q}\}, \mathbb{E}\{\chi_{\mathcal{C}_q}\} \leq 1$.

It remains to bound $\mathbb{E}\{1 - \chi_{\mathcal{C}_q}\}$; i.e., $\mathbb{P}(\mathcal{C}_q^c)$ (cf. (72)), where $\mathbb{P}(\cdot)$ is the probability measure. Beginning with $\mathbb{P}(\mathcal{A}_q^c)$, we derive a bound on $\cos^2(\xi_q)$. Consider, $\hat{\mathbf{p}}_q = \cos(\phi_q)\mathbf{p}_q + \sin(\phi_q)\mathbf{g}_q$, and note that \mathbf{p}_q (cf. (6)) can be seen as the projection of $\hat{\mathbf{h}}_q$ into the orthogonal complement of $\mathcal{H}_{-q} = \text{span}(\hat{\mathbf{h}}_1, \dots, \hat{\mathbf{h}}_{q-1}, \hat{\mathbf{h}}_{q+1}, \dots, \hat{\mathbf{h}}_Q)$; after being normalized; that is, $\mathbf{p}_q = \frac{\mathbf{P}_{\mathcal{H}_{-q}}^\perp \hat{\mathbf{h}}_q}{\|\mathbf{P}_{\mathcal{H}_{-q}}^\perp \hat{\mathbf{h}}_q\|}$. We further express $\hat{\mathbf{h}}_q$ as $\hat{\mathbf{h}}_q = V_1 \mathbf{p}_q + V_2 \frac{\mathbf{P}_{\mathcal{H}_{-q}}^\perp \hat{\mathbf{h}}_q}{\|\mathbf{P}_{\mathcal{H}_{-q}}^\perp \hat{\mathbf{h}}_q\|}$, where $V_1 \sim \Gamma(N_t - Q + 1, 1)$, $V_2 \sim \Gamma(Q - 1, 1)$ and denote $W_q = \cos^2(\angle(\hat{\mathbf{h}}_q, \mathbf{p}_q))$. It therefore follows that $\sqrt{W_q} = \frac{V_1^2}{V_1^2 + V_2^2} \sim \beta(MN_t - Q + 1, Q - 1)$ [36]. Combining the latter representations of $\hat{\mathbf{p}}_q$ and $\hat{\mathbf{h}}_q$ one obtains $\cos^2(\xi_q) = |\hat{\mathbf{h}}_q^\dagger \hat{\mathbf{p}}_q|^2 = |\sin(\phi_q) \hat{\mathbf{h}}_q^\dagger \mathbf{g}_q + \cos(\phi_q) \hat{\mathbf{h}}_q^\dagger \mathbf{p}_q|^2 \geq -|\sin(\phi_q) \hat{\mathbf{h}}_q^\dagger \mathbf{g}_q|^2 + |\cos(\phi_q) \sqrt{W_q}|^2 \geq \cos^2(\phi_q) W_q - \sin^2(\phi_q)$

Now to $\mathbb{P}(\mathcal{A}_q)$. Consider $\mathbb{P}(\mathcal{A}_q^c) = \mathbb{P}(\xi_q > \frac{\pi}{2} - \theta_q) = \mathbb{P}(\cos^2(\xi_q) \leq \sin^2(\theta_q))$, then $\mathbb{P}(\mathcal{A}_q^c) \leq \mathbb{P}(\cos^2(\phi_q) W_q - \sin^2(\phi_q) \leq \sin^2(\theta_q)) \leq \mathbb{P}(W_q \leq \sin^2(\theta_q) + 2\sin^2(\phi_q))$, where in the latter we used $\cos^2(\phi_q) = 1 - \sin^2(\phi_q)$ and $0 \leq W_q \leq 1$. Let $Y_q = \sin^2(\theta_q) + 2\sin^2(\phi_q)$ and let $F_{Y_q[y]} = \mathbb{P}(Y_q \leq y)$, then, $\mathbb{P}(\mathcal{A}_q^c) \leq \mathbb{P}(W_q \leq Y_q) = \int \mathbb{P}(W_q \leq y | Y_q = y) dF_{Y_q}(y) = \mathbb{E}\{\mathbb{P}(W_q \leq y | Y_q = y)\}$. Since W_q is independent of θ_q and ϕ_q , $\mathbb{P}(W_q \leq y | Y_q = y) = I_y(MN_t - Q + 1, Q - 1)$ where I_y is the regularized beta function. Using $I_y(MN_t - Q + 1, Q - 1) \leq y$ for $0 \leq y \leq 1$, one obtains $\mathbb{P}(\mathcal{A}_q^c) \leq \mathbb{E}\{Y_q\} = \mathbb{E}\{\sin^2(\theta_q) + 2\sin^2(\phi_q)\}$. Next, similar to (74) it can be shown that $\mathbb{P}(\mathcal{A}_q^c) \leq 3(\mathcal{U}(2^{B/Q}, a) + \mathcal{V}_M(2^{B/Q}, a))$, where a, \mathcal{U} and \mathcal{V}_M are defined in Theorem 1. To complete the proof, we bound $\mathbb{P}(\mathcal{C}_q^c)$ as follows $\mathbb{P}(\mathcal{C}_q^c) = \mathbb{P}((\mathcal{A}_q \cup \mathcal{B}_q)^c) \leq \mathbb{P}(\mathcal{A}_q^c \cup \mathcal{B}_q^c) \leq \mathbb{P}(\mathcal{A}_q^c) + \mathbb{P}(\mathcal{B}_q^c)$. Finally, similar to $\mathbb{P}(\mathcal{A}_q^c)$, it can be shown that $\mathbb{P}(\mathcal{B}_q^c) \leq 3((\mathcal{U}(2^{B/Q}, a) + \mathcal{V}_M(2^{B/Q}, a))$, which establishes the desired result.

APPENDIX D

The proof of Lemma 7, is very similar to that of Lemma 3 (cf. Appendix C). It is obtained by substituting $\tilde{\mathbf{h}}_q, \hat{\mathbf{h}}_q, \tilde{\mathbf{p}}_j, \hat{\mathbf{p}}_j, M_q, \tilde{P}, \tilde{N}_t, \tilde{a}, B/(Q - \bar{Q})$ for $\mathbf{h}_q, \hat{\mathbf{h}}_q, \mathbf{p}_j, \hat{\mathbf{p}}_j, M, P, N_t, a, B/Q$, respectively, in Appendix C, and following similar steps.

REFERENCES

- [1] N. Arad and Y. Noam, “Precode and quantize channel state information sharing for cloud radio access networks,” *IEEE Int. Conf. Commun. (ICC)*, pp. 1–6, 2018.
- [2] D. Gesbert, S. Hanly, H. Huang, S. Shamai Shitz, O. Simeone, and W. Yu, “Multi-cell MIMO cooperative networks: A new look at interference,” *IEEE J. Sel. Areas Commun.*, vol. 28, pp. 1380–1408, December 2010.
- [3] I. Chih-Lin, C. Rowell, S. Han, Z. Xu, G. Li, and Z. Pan, “Toward green and soft: a 5G perspective,” *IEEE Commun. Mag.*, vol. 52, no. 2, pp. 66–73, 2014.

- [4] A. Checko, H. L. Christiansen, Y. Yan, L. Scolari, G. Kardaras, M. S. Berger, and L. Dittmann, "Cloud RAN for mobile networks - a technology overview," *IEEE Commun. Surveys & Tutorials*, vol. 17, no. 1, pp. 405–426, 2015.
- [5] U. Dötsch, M. Doll, H.-P. Mayer, F. Schaich, J. Segel, and P. Sehier, "Quantitative analysis of split base station processing and determination of advantageous architectures for LTE," *Bell Labs Tech. J.*, vol. 18, no. 1, pp. 105–128, 2013.
- [6] D. Wubben, P. Rost, J. S. Bartelt, M. Lalam, V. Savin, M. Gorgoglione, A. Dekorsy, and G. Fettweis, "Benefits and impact of cloud computing on 5G signal processing: Flexible centralization through cloud-RAN," *IEEE signal process. mag.*, vol. 31, no. 6, pp. 35–44, 2014.
- [7] J. Bartelt, P. Rost, D. Wubben, J. Lessmann, B. Melis, and G. Fettweis, "Fronthaul and backhaul requirements of flexibly centralized radio access networks," *IEEE Wireless Commun.*, vol. 22, no. 5, pp. 105–111, 2015.
- [8] 3GPP TR 38.300, *New Radio; Overall description; Stage-2*, 9 2017. V1.0.0, pages 13-14.
- [9] N. Jindal, "MIMO broadcast channels with finite-rate feedback," *IEEE Trans. Inf. Theory*, vol. 52, pp. 5045–5060, Nov 2006.
- [10] G. Caire, N. Jindal, M. Kobayashi, and N. Ravindran, "Multiuser MIMO achievable rates with downlink training and channel state feedback," *IEEE Trans. Inf. Theory*, vol. 56, June 2010.
- [11] Y. Noam and B. M. Zaidel, "On the two-user MISO interference channel with single-user decoding: Impact of imperfect CSIT and channel dimension reduction," *IEEE Trans. Signal Process.*, vol. 67, no. 10, 2019.
- [12] D. Jaramillo-Ramirez, M. Kountouris, and E. Hardouin, "Coordinated multi-point transmission with imperfect CSI and other-cell interference," *IEEE Trans. Wireless Commun.*, vol. 14, no. 4, pp. 1882–1896, 2015.
- [13] B. Makki, J. Li, T. Eriksson, and T. Svensson, "Throughput analysis for multi-point joint transmission with quantized CSI feedback," in *Veh. Technol. Conf. (VTC Fall), 2012 IEEE*, pp. 1–5, IEEE, 2012.
- [14] S. Yu, H.-B. Kong, Y.-T. Kim, S.-H. Park, and I. Lee, "Novel feedback bit allocation methods for multi-cell joint processing systems," *IEEE Trans. Wireless Commun.*, vol. 11, no. 9, pp. 3030–3036, 2012.
- [15] B. Dai and W. Yu, "Sparse beamforming for limited-backhaul network MIMO system via reweighted power minimization," in *Global Commun. Conf. (GLOBECOM), 2013 IEEE*, pp. 1962–1967, IEEE, 2013.
- [16] R. Zakhour and D. Gesbert, "Optimized data sharing in multicell MIMO with finite backhaul capacity," *IEEE Trans. Signal Process.*, vol. 59, no. 12, pp. 6102–6111, 2011.
- [17] O. Simeone, O. Somekh, H. V. Poor, and S. Shamai, "Downlink multicell processing with limited-backhaul capacity," *EURASIP J. Adv. Signal Process.*, vol. 2009, no. 1, p. 840814, 2009.
- [18] S.-H. Park, O. Simeone, O. Sahin, and S. Shamai, "Joint precoding and multivariate backhaul compression for the downlink of cloud radio access networks," *IEEE Trans. Signal Process.*, vol. 61, pp. 5646–5658, 2013.
- [19] J. Kang, O. Simeone, J. Kang, and S. S. Shitz, "Joint signal and channel state information compression for the backhaul of uplink network MIMO systems," *IEEE Trans. Wireless Commun.*, vol. 13, 2014.
- [20] D. Wang, Y. Wang, R. Sun, and X. Zhang, "Robust C-RAN precoder design for wireless fronthaul with

imperfect channel state information,” in *Wireless Commun. Netw. Conf. (WCNC)*, pp. 1–6, IEEE, 2017.

[21] T. R. Lakshmana, A. Tölli, R. Devassy, and T. Svensson, “Precoder design with incomplete feedback for joint transmission,” *IEEE Trans. Wireless Commun.*, vol. 15, no. 3, pp. 1923–1936, 2016.

[22] S. Zhou, J. Gong, and Z. Niu, “Distributed adaptation of quantized feedback for downlink network MIMO systems,” *IEEE Trans. Wireless Commun.*, vol. 10, no. 1, pp. 61–67, 2011.

[23] A. Papadogiannis, H. J. Bang, D. Gesbert, and E. Hardouin, “Efficient selective feedback design for multicell cooperative networks,” *IEEE Trans. Veh. Technol.*, vol. 60, no. 1, pp. 196–205, 2011.

[24] Y. Shi, J. Zhang, and K. B. Letaief, “CSI overhead reduction with stochastic beamforming for cloud radio access networks,” in *IEEE Int. Conf. Commun. (ICC)*, pp. 5154–5159, IEEE, 2014.

[25] W. Santipach and M. L. Honig, “Signature optimization for CDMA with limited feedback,” *IEEE Trans. Inf. Theory*, vol. 51, no. 10, pp. 3475–3492, 2005.

[26] M. Kountouris and J. G. Andrews, “Downlink SDMA with limited feedback in interference-limited wireless networks,” *IEEE Trans. Wireless Commun.*, vol. 11, no. 8, pp. 2730–2741, 2012.

[27] A. J. Goldsmith, *Wireless Communications*. Cambridge university press, 2005.

[28] R. Zhang, “Cooperative multi-cell block diagonalization with per-base-station power constraints,” *IEEE J. Sel. Areas Commun.*, vol. 28, no. 9, pp. 1435–1445, 2010.

[29] X. Yu, W. Xu, S. H. Leung, Q. Shi, and J. Chu, “Power allocation for energy efficient optimization of distributed MIMO system with beamforming,” *IEEE Trans. Veh. Technol.*, vol. 68, pp. 8966–8981, 2019.

[30] D. A. Basnayaka, P. J. Smith, and P. A. Martin, “Performance analysis of dual-user macrodiversity MIMO systems with linear receivers in flat Rayleigh fading,” *IEEE Trans. Wirel. Commun.*, vol. 11, no. 12, 2012.

[31] D. A. Basnayaka, P. J. Smith, and P. A. Martin, “Performance analysis of macrodiversity MIMO systems with MMSE and ZF receivers in flat rayleigh fading,” *IEEE Trans. Wirel. Commun.*, vol. 12, 2013.

[32] R. Senanayake, P. L. Yeoh, and J. Evans, “On the sum capacity of cluster-based cooperative cellular networks,” in *IEEE Int. Conf. Commun.*, pp. 1613–1618, sep 2015.

[33] 3GPP TR 36.814, *E-UTRA; Further advancements for E-UTRA physical layer aspects*, 3 2010. V9. page 61.

[34] N. Ravindran and N. Jindal, “Limited feedback-based block diagonalization for the MIMO broadcast channel,” *IEEE Journal on Selected Areas in Communications*, vol. 26, pp. 1473–1482, October 2008.

[35] A. H. David and H. N. Nagaraja, *Order Statistics*. N. J.: John Wiley, third ed., 2003.

[36] J. C. Roh and B. D. Rao, “Transmit beamforming in multiple-antenna systems with finite rate feedback: a VQ-based approach,” *IEEE Trans. Inf. Theory*, vol. 52, no. 3, pp. 1101–1112, 2006.

[37] M. S. Alouini and A. J. Goldsmith, “Capacity of Rayleigh fading channels under different adaptive transmission and diversity-combining techniques,” *IEEE Trans. Veh. Technol.*, vol. 48, no. 4, pp. 1165–1181, 1999.

[38] C. K. Au-Yeung and D. J. Love, “On the performance of random vector quantization limited feedback beamforming in a miso system,” *IEEE Transactions on Wireless Communications*, vol. 6, no. 2, 2007.

SUPPLEMENTARY MATERIAL

A DERIVATION OF (18)

To show (18) we use the formula for the maximum ratio combining (MRC) capacity (cf. [37]). Note that under no quantization error, $\text{SINR}_q(\{\mathbf{p}_i^*\}_{i \in \mathcal{Q}}) = P|\mathbf{h}_q^\dagger \mathbf{p}_q^*|^2 = P\|\mathbf{h}_q^{\text{ZF}}\|^2$, where $\mathbf{h}_q^{\text{ZF}} = (\mathbf{N}_q^*)^\dagger \mathbf{h}_q$ and $\mathbf{N}_q^* \in \mathbb{C}^{MN_t \times T}$ is an orthonormal basis for the null space of $\{\mathbf{h}_j\}_{j \in \mathcal{Q}_{-q}}$. Because \mathbf{N}_q^* is independent of \mathbf{h}_q , with independent columns and $\alpha_{q,m} = 1/M$, it follows that $\mathbf{h}_q^{\text{ZF}}/\sqrt{M} \sim \mathcal{CN}(\mathbf{0}_T, \mathbf{I}_T)$ and therefore, R_q^* in (11) is equal to the rate obtained with maximum ratio-combining of a single-user Rayleigh fading MISO channel of dimensionality T and power P/M . By [38, Lemma 4] the latter rate is given by (18).

B PROOF OF COROLLARY 8

We begin with showing that

$$M_q = (1 - \bar{Q}/Q)M, \forall q \in \mathcal{Q} \quad (\text{S.1})$$

and

$$\sum_{j \in \mathcal{Q}_{-q}} \frac{M_{q,j}}{M_j} = (Q - \bar{Q} - 1). \quad (\text{S.2})$$

Define $L \triangleq Q/M \in \mathbb{N}$, $r \triangleq \bar{Q}/Q$ and note that $rM \in \mathbb{N}$. Without loss of generality, consider $q = 1$ and assume that $\mathcal{Q}_m = \{(m-1)L+1, \dots, mL\}$ for $m \in \mathcal{M}$. From Definition 7, MS-1 is not served by S-RRH-1, … S-RRH- Mr , therefore $M_1 = M(1-r)$ which establishes (S.1). To show (S.2), we note that $\forall j \in \mathcal{Q}_1$, MS- j is served by the same set of S-RRHs as MS-1; thus, $M_{1,j} = M_1, \forall j \in \mathcal{Q}_1$. Assume, for now, that $0 \leq r \leq \frac{1}{2}$; then by the symmetric selection policy $M_{1,j} = M_1 - k \forall j \in \{\mathcal{Q}_{(1+k) \bmod M} \cup \mathcal{Q}_{(1-k) \bmod M} : k = 1, \dots, Mr\}$ and $M_{1,j} = M_1 - Mr \forall j \in \{\mathcal{Q}_{(k \bmod M)+1} \cup \mathcal{Q}_{(-k \bmod M)+1} : k = Mr+1, \dots, \lfloor M/2 \rfloor\}$. Thus

$$\sum_{i=2}^Q M_{1,i} = (L-1)M_1 + L[(M-2Mr-1)(M_1-Mr) + Mr(-Mr+2M_1-1)]. \quad (\text{S.3})$$

Now to the case where $r > \frac{1}{2}$. Here $M_{1,j} = M_1, \forall j \in \mathcal{Q}_1$,

$$M_{1,j} = M_1 - k \forall j \in \{\mathcal{Q}_{(k \bmod M)+1} \cup \mathcal{Q}_{(-k \bmod M)+1} : k = 1, \dots, M_1-1\} \quad (\text{S.4})$$

and $M_{1,j} = 0$ otherwise. Thus,

$$\sum_{i=1}^Q M_{1,i} = (L-1)M_1 + L(M_1-1)M_1. \quad (\text{S.5})$$

Substituting $L = Q/M$, $M_1 = M(1-r)$ and $r = \bar{Q}/Q$ in both (S.3), (S.5) it follows that the two expressions are identical and are given by

$$\sum_{i=2}^Q M_{1,i} = \frac{M(Q-\bar{Q}-1)(Q-\bar{Q})}{Q} \quad (\text{S.6})$$

which establishes (S.1) and (S.2). It remains to calculate $\tilde{T}_q = M_q \tilde{N}_t - \tilde{Q}_q + 1$. Recalling that $M_q = M(1-r)$, it is sufficient to calculate \tilde{Q}_q , which is given by

$$\tilde{Q}_q = Q - \sum_{j \in \mathcal{Q}_{-q}} \chi_{\{0\}}(M_{q,j}) \quad (\text{S.7})$$

Note that $\sum_{j \in \mathcal{Q}_{-q}} \chi_{\{0\}}(M_{q,j})$ can be written as $|\{j, |\mathcal{M}_{q,j}| = 0, j \neq q\}|$; i.e, the number of MSs served by at least one S-RRH that serves MS- q . For $r \geq \frac{1}{2}$, the latter sum is equal to $2Q(1-r) - L - 1$, whereas for $r < 1/2$, $\tilde{Q}_q = Q - 1$. This can be written as, $\tilde{Q}_q = Q - \min(Q, -2\bar{Q} + (2 - 1/M)Q - 1)$, and therefore

$$\tilde{T}_q = M(1-r)\tilde{N}_t + 1 - \min\left[Q, \left(2 - \frac{1}{M}\right)Q - 2\bar{Q}\right] \quad (\text{S.8})$$

which establishes the desired result.

C A DETAILED DESCRIPTION OF THE SIMULATION SETUP

We now provide a detailed description of the two simulation setups considered in section VI.

A. Symmetric Setup: Figure 2

Here we consider a network satisfying Assumption 8 under the symmetric system policy of Definition 7, with four S-RRHs and eight MSs. We begin with evaluating the standard ZF scheme for two transmitter-SNRs levels; i.e., we set P according to Assumption 6 with $P_{\max} = 15$ dB and $P_{\min} = 35$ dB, and the noise power to one. Fig. 2(a) depicts the standard-scheme performance, evaluated via MC, compared to the rate lower-bound $\hat{R} \geq R^* - (\Delta\bar{R}_1 + \Delta\bar{R}_2)$ (cf. Remark 4), where $\Delta\bar{R}_1, \Delta\bar{R}_2$ are given in Theorem 1 and R_q^* in (18). Due to the symmetric setup, the bound is not a function of q . Also included is the rate under perfect CSI, (cf. (18)). We used 300 channel realizations for each B to evaluate the ergodic rate for every $N_t \in \{2, \dots, 8\}$, and

then picked the N_t with the maximum rate. By doing so, we considered that transmitters could always turn off some of their antennas if it yields a higher rate. The corresponding bound was also maximized over N_t for each B .

Fig. 2(b) studies the P&Q and the standard schemes for $M = 4$ and $Q = 8$. It depicts the bound of the latter scheme, as in Fig. 2(a) compared to the corresponding bound of the P&Q; i.e., $\hat{\bar{R}} \geq R^* - (\Delta\bar{R}_1 + \Delta\bar{R}_2 + \Delta R_{AG})$ (cf. Remark 4), where $\Delta\bar{R}_1, \Delta\bar{R}_2, \Delta R_{AG}$ are given in Corollary 8 and R^* in (18). The bounds are collated to $\hat{\bar{R}}$ and \hat{R} , obtained via MC. We set $P_{\max} = 35$ dB, and P according to Assumptions 6 and 7 for the standard and P&Q schemes, respectively. Explicitly, for each B , we evaluated the rate for all feasible values of \bar{Q} (in this symmetric setup, $\bar{Q} \in \{0, 2, 4, 6\}$) for every $N_t = \{2, \dots, 8\}$.¹⁶ We then picked the maximum over \bar{Q} and subsequently took the maximum over N_t . As in Fig. 2(a) we used 300 channel realizations. The corresponding bound were maximized similarly.

B. Randomly Distributed MSs: Figure 3

Here we consider a practically oriented setup with randomly dispersed MSs while considering propagation loss and shadowing. The setup includes a cluster of $M = 4$ S-RRHs, each placed at the center of one of four adjacent hexagons, creating a hexagonal grid with an edge-length of 100 m; i.e., we cut four hexagons and placed an S-RRH at the center of each hexagon. Each S-RRH is equipped with $N_t = 8$ isotropic transmit antennas. Eight single-antenna MSs ($Q = 8$) were placed uniformly at random in the area spanned by the hexagons, with a minimum distance of 10 m between each MS and S-RRH. The results were averaged over 20 realizations of MS-placements, where each realization determined a set of attenuation factors $\alpha = \{\alpha_{q,m} : q = 1 \dots 8, m = 1 \dots 4\}$ according $\alpha_{q,m} = -128 - 37.6 \log_{10}(r_{q,m})$ (in dB),¹⁷ where $r_{q,m}$ is the distance from S-RRH- m to MS- q in Km. The noise level at the receivers was -121 dBm. For each realization α , we calculated the rates $\hat{R}_q(\alpha), \hat{\bar{R}}_q(\alpha)$ using (10) and Definition 5, for the corresponding scheme,¹⁸ by averaging over 40 realizations of $\{\mathbf{h}_{q,m}\}_{q \in \mathcal{Q}, m \in \mathcal{M}}$, generated according to Assumption 1. The network throughput for a given α was calculated as $\bar{R}(\alpha) =$

¹⁶Note that for $\bar{Q} = 0$, the P&Q coincides with the standard scheme.

¹⁷This model was used for urban-area non-line-of-site links by the 3GPP; cf. page 61 3GPP Technical Report 36.814 [33].

¹⁸ $\hat{R}_q(\alpha)$ is a function of α by (9) and by Assumption 1.

$1/Q \sum_{q=1}^Q \hat{R}_q(\boldsymbol{\alpha})$, and the throughput \bar{R} was calculated by averaging $\bar{R}(\boldsymbol{\alpha})$ over 20 realizations of $\boldsymbol{\alpha}$; i.e., $\bar{R} = 1/20 \sum_{i=1}^{20} \bar{R}(\boldsymbol{\alpha}_i)$, where each $\boldsymbol{\alpha}_i$ corresponded to a different MS placement. $\bar{R}(\boldsymbol{\alpha})$ and \bar{R} are defined similarly.

To ensure a fair comparison, in all figures (Figures 3(a) and 3(b)) we considered that the transmitters could always turn off some of their antennas to reduce the effective MISO channel dimensions. Therefore, in the standard scheme, for each $\boldsymbol{\alpha}$, we evaluated $\bar{R}(\boldsymbol{\alpha})$ for $N_t = \{2, \dots, 8\}$ and picked the maximum. We applied a similar procedure for the P&Q scheme, where we maximized the rate over \bar{Q} , with $N_t = 8$; i.e., by evaluating $\bar{R}(\boldsymbol{\alpha})$ for $\bar{Q} = \{1, \dots, 6\}$ and taking the maximum.

Finally, we used the following power allocation strategy.

Definition 8 (The equal power-backoff strategy): Considering the standard feedback scheme, each S-RRH transmits with equal power to each MS; i.e., $P_{q,m} = P, \forall q \in \mathcal{Q}, m \in \mathcal{M}$. To avoid violating its individual power constraint P_{\max} , each S-RRH sets $P = \frac{\gamma P_{\max}}{Q}$, where $\gamma \geq 1$ is the backoff factor, given by

$$\gamma = \min \left\{ \gamma_m : \sum_{q \in \mathcal{Q}} \gamma_m \|\mathbf{p}_{q,m}\|^2 = Q, m \in \mathcal{M} \right\} \quad (\text{S.9})$$

To explain this strategy, we note that $E\{\|\mathbf{x}_m\|^2 | U\} = \sum_{q \in \mathcal{Q}} \frac{P_{\max}}{Q} \|\mathbf{p}_{q,m}\|^2 \leq P_{\max}$, and therefore $\sum_{q \in \mathcal{Q}} \|\mathbf{p}_{q,m}\|^2 \leq Q, \forall m \in \mathcal{M}$. Because $\|\mathbf{p}_q\| = 1$, the latter constraint is always satisfied with strong inequality, implying that it is possible to increase the power. The objective of (S.9) is to guarantee that at least one S-RRH transmits with maximal power.¹⁹ Considering the P&Q scheme, the strategy in Definition 8 applies with a minor modification. Each S-RRH serves exactly $Q - \bar{Q}$ MSs, with power $\tilde{P}_{q,m} = \tilde{P} = \frac{\tilde{\gamma} P_{\max}}{Q - \bar{Q}}, \forall q \in \mathcal{Q}, m \in \mathcal{M}$, where $\tilde{\gamma}$ is defined similarly to (S.9) while substituting $\tilde{\mathbf{p}}_{q,m}$ for $\mathbf{p}_{q,m}$ and $Q - \bar{Q}$ for Q .

Fig. 3(a) presents the throughput as a function of each S-RRH transmit power, P_{\max} (cf. Assumption 2). Figure 3(b) presents the average throughput as a function of B , under a per-S-RRH power constraint of $P_{\max} = 45$ dBm.

¹⁹Note that while this power allocation strategy is not optimal, it yields good performance in high SNRs.